OPTIMISATION OF KAOLIN BIOLEACHING USING SURFACE, CHEMICAL AND STRUCTURAL STUDIES

PANG JUN HAO

Universiti Tunku Abdul Rahman

OPTIMISATION OF KAOLIN BIOLEACHING USING SURFACE, CHEMICAL AND STRUCTURAL STUDIES

PANG JUN HAO

A project report submitted in partial fulfilment of the requirements for the award of Bachelor of Mechanical Engineering with Honours

Lee Kong Chian Faculty of Engineering and Science
Universiti Tunku Abdul Rahman

April 2024

DECLARATION

I hereby declare that this project report is based on my original work except for citations and quotations which have been duly acknowledged. I also declare that it has not been previously and concurrently submitted for any other degree or award at UTAR or other institutions.

Signature : _____

Name : Pang Jun Hao

ID No. : 2000910

Date : 28/04/2023

APPROVAL FOR SUBMISSION

I certify that this project report entitled **"OPTIMISATION OF KAOLIN BIOLEACHING USING SURFACE, CHEMICAL AND STRUCTURAL CHANGE OF KAOLIN"** was prepared by **PANG JUN HAO** has met the required standard for submission in partial fulfilment of the requirements for the award of Bachelor of Mechanical Engineering with Honours at Universiti Tunku Abdul Rahman.

Approved by,

Signature : 

Supervisor : Dr. Kuan Seng How

Date : 28/04/2023

Signature :

Co-Supervisor :

Date :

ACKNOWLEDGEMENTS

I would like to thank everyone who had contributed to the successful completion of this project. I would like to express my gratitude to my research supervisor, Dr. Kuan Seng How for his invaluable advice, guidance and his enormous patience throughout the development of the research.

In addition, I would also like to express my gratitude to my loving parents and friends who had helped and given me encouragement. In this project, I would like to thank my senior Monisha A/P Rajamohan who guided me in conducting the experiments, and facilities provided by Universiti Kebangsaan Malaysia and Universiti Tunku Abdul Rahman. I would also like to thank my senior Muhammad Ahmad Zan who guided me in conducting the experiments in UKM and sometimes solved my transportation problem.

ABSTRACT

Kaolin, a valuable clay mineral used in ceramics, whiteware manufacturing, and refractories, faces challenges due to iron impurities affecting its properties and colouration. Conventional methods for iron removal are not sustainable, necessitating eco-friendly alternatives like bioleaching with Bacillus Cereus. This study focuses on exploring how nutrients, particularly yeast and yeast with glucose solution, impact bioleaching efficiency within 10 days of the experiment. This study investigates the morphological, chemical, and structural alterations of kaolin during bioleaching using Bacillus cereus. By analyzing experimental outcomes, it was determined that a combination of yeast extract and glucose solution serves as the optimal nutrient source for enhancing bioleaching efficiency. Phenanthroline analysis revealed a significant increase in Fe (II) concentration from 1.06 µg/ml on day 0 to 3.78 µg/ml on day 10. Energy-dispersive X-ray spectroscopy (EDS) further demonstrated a bioleaching efficiency of 54.88% in batch 1 and 51.55% in batch 2, surpassing previous studies, likely attributable to the selected nutrient types. Surface analysis via scanning electron microscopy (SEM) indicated heightened crystallinity in the kaolin structure post-bioleaching. Remarkably, the chemical composition and bonds of kaolin remained unaltered, as confirmed by X-ray diffraction (XRD) and Fourier-transform infrared spectroscopy (FTIR). This study successfully achieves its objectives and suggests further laboratory-scale optimization to facilitate scale-up. Future investigations will delve into optimizing nutrient types using various *Bacillus* species to maximize bioleaching efficiency, thereby contributing to the sustainable utilization of kaolin resources. While the nutrient source can be the catalyst to accelerate the progress, different bacteria will have their optimum condition. To further increase the efficiency, other bacteria types rather than *Bacillus* species can be investigated because the rate of metabolism rate for each bacteria is different, then the duration of bioleaching is also different.

TABLE OF CONTENTS

LIST OF TABLES

LIST OF FIGURES

LIST OF SYMBOLS / ABBREVIATIONS

w/v	weight/ volume concentration, %
A. niger	*Aspergillus niger*
Bacillus. sp	*Bacillus* species
B. aryabhattai	*Bacillus aryabhattai*
B. cereus	*Bacillus cereus*
B. megaterium	*Bacillus megaterium*
S. oneidensis	*Shewanella oneidensis*
S. putrefaciens	*Shewanella putrefaciens*
Fe	Iron
NH_3	Ammonia
EDS	Energy Dispersive X-ray
EPS	Extracellular Polymeric Substances
FTIR	Fourier Transform Infrared Spectroscopy
ICP-OES	Inductively Coupled Plasma Optical Emission Spectroscopy
rRNA	Ribosomal Ribonucleic acid
SEM	Scanning Electron Microscopy
XRD	X-ray diffraction
D0	Day 0
D10	Day 10

LIST OF APPENDICES

CHAPTER 1

INTRODUCTION

1.1 Background

Kaolin is a soft white clay mineral composed primarily of the mineral kaolinite, $Al_2Si_2O_5(OH)_4$. The theoretical chemical composition of kaolinite is 39.50% - Al_2O_3, 46.54% - SiO_2 and 13.96% - H_2O (Scorzelli et al., 2010). While kaolinite can exist in a nearly pure form, it often contains impurities that can significantly impact its characteristics and quality.

Kaolin is extensively used in the ceramic industry due to its high fusion temperature and white-burning characteristics, making it ideal for producing whiteware such as whiteware and porcelain, as well as refractories (Bhutia et al., 2019). In whiteware manufacturing, kaolin is typically blended with nearly equal amounts of silica and feldspar, along with a smaller quantity of plastic light-burning clay called ball clay.

Kaolin is also used in pigment, paper, and filler manufacturing. Its natural white colour and fine particle size make it an excellent extender and opacifier in pigmented formulations (Buyondo, Kasedde and Kirabira, 2022). In paper and filler industries, kaolin is used to improve the smoothness, brightness, and opacity to enhance the print quality for cost reduction (Bundy and Ishley, 1991).

However, among these impurities, iron content and titanium content are notable (Department of Jobs, 2021). Iron can be present in the form of minerals like pyrite, limonite, hematite, rutile, and others. The iron content directly influences the whiteness index and the overall appearance of the final kaolin product. High iron content can result in a brownish or reddish hue in the clay, which is undesirable in many applications, such as ceramics, where the desired colour is typically white (Lee et.al 2002). Furthermore, the presence of iron can adversely affect the dielectric properties and chemical stability of ceramics (Tracy, 2018).

Hence the leaching of kaolin is necessary, it can be leached with the method of chemical, physical and biological. The utilization of chemical treatment comes with high costs, and potential hazards, and necessitates

specialized storage and operational conditions, especially the sodium hydrosulfite (Zegeye et al., 2013). They are often costly, complex, and environmentally harmful (Groudev, 1987).

This underscores the ongoing need for research and development efforts to explore more sustainable and eco-friendly alternatives for iron removal from kaolin, with an emphasis on reducing energy consumption and waste production while maintaining product quality. So, the biological method fulfils the requirement and is sustainable as compared to physical and chemical treatments (Zegeye et al., 2013). In this study, the biological method will be investigated to optimise the efficiency of iron removal.

1.2 Importance of the Study

This study may provide the optimization of the bioleaching process of the *Bacillus* species bacteria. *Bacillus.* species is widely used as a bacteria for bioleaching because it is the most effective for metal solubilization (Admin, 2021). The effectiveness of the *Bacillus* species and its optimum condition for bioleaching may provide a solution to a higher extraction of iron from kaolin or valuable insight for further research on the bioleaching of the *Bacillus* species. Resulting in a better-quality kaolin from biological methods to be utilised in different applications.

It is important to provide research results based on the increase in the quality of kaolin through the reduction of iron content. This is why this report presents the investigation of kaolin clay leaching though biological methods to find the optimum experimental conditions.

1.3 Problem Statement

Reducing iron content in kaolin is essential for enhancing its quality for industrial applications such as ceramics and paper manufacturing. Conventional methods like froth flotation, gravity separation, magnetic separation, reductive roasting, and acid treatment are commonly used to improve kaolin's whiteness and purity by removing iron-bearing impurities (Guo et al., 2010a). However, these methods are energy-intensive, costly, and generate substantial waste, posing significant environmental concerns.

According to Scorzelli et al. (2008), the research has shown that combining magnetic separation with chemical bleaching achieves high whiteness indices, but these processes still involve the use of harmful chemicals that require treatment before disposal. Alternatively, bioleaching using iron-reducing bacteria offers a more environmentally friendly solution (HALVORSON and STARKEY, 1927, pp.381–402). These bacteria metabolize iron impurities, potentially reducing ecological impact and production costs.

Previous research on bioleaching has not fully optimized its use for large-scale industrial applications, particularly in the case of kaolin. This method takes longer compared to alternatives, posing a challenge for industries where time is critical for production. The inconsistency in iron extraction through bioleaching remains unclear in past studies. Therefore, this report's literature review will delve into bioleaching mechanisms and explore optimal nutrient conditions for improvement.

1.4 Objectives

The objectives of this project are:

1. To measure the iron reduction efficiencies of *Bacillus cereus* in kaolin substrate.
2. To determine the effect of carbon and nitrogen nutrient sources on iron reduction efficiency.
3. To analyse the changes in surface morphology, structure and chemical composition of kaolin before and after bioleaching.

1.5 Scope and Limitation of the Study

This project will focus on the surface, structure and chemical characterisation of kaolin before and after bioleaching as described in Chapter 4. *Bacillus* species will be used because it continues the investigation from previous studies (Lee et al., 2023).

The project will not measure the changes for every day of bioleaching due to limitations in manpower and funding. The project will not focus on the atomic or nanoscale characterisation of changes in kaolin due to limitations in equipment. The project will not use the whiteness index to characterise kaolin

due to the lack of a colourimeter at the UTAR laboratories. The project will not use the ICP-OES to have the elemental analysis because it is under maintenance.

Furthermore, only one of the *Bacillus* species will be used, it is *B.cereus.* It is because of the time constraint and lack of raw kaolin powder to continue the further experiment with the different nutrient sources.

1.6 Contribution of the Study

This study contributes to enhancing environmental sustainability by reducing chemical waste and assessing the feasibility of replacing conventional iron extraction from kaolin with bioleaching. It explores the capability of *Bacillus* species bacteria to leach iron as an alternative method. Additionally, the investigation delves into the leaching mechanism, offering insights into adjusting leaching times by understanding how bacteria bind to iron impurities in kaolin. This may lead to better control over the leaching process.

1.7 Outline of the Report

This report consists of five chapters, Chapter 1 introduces the report and covers the background information, importance of the study, problem statement, aim and objectives, scope and limitations along with the contribution of the study to provide a basic understanding of bioleaching, the necessity for alternatives to conventional iron leaching methods and the benefits of bioleaching to environment.

Chapter 2 is the literature review which covers the literature reviews of the previous research and provides a basis for the study and experiments. The factors and ways to optimise bioleaching as well as the methodologies involved. A summary table is arranged to have a clear insight into the result from different factors.

Chapter 3 explains the methodology of the experiment with the flow of the experiment, chemicals and materials required and their usage. It also specifies the equipment and necessary settings for the experiments. Chapter 4 presents the results and discusses their implications, comparing them with previous studies to offer readers a deeper insight. Finally, Chapter 5 concludes the findings from the experiments and recommendations for future work.

CHAPTER 2

LITERATURE REVIEW

2.1 Introduction

Kaolin, a clay mineral abundant in nature, has gained attention due to its potential as a source of valuable materials. Depending on the source and depositional environment, raw kaolin usually contains quartz, anatase, rutile, pyrite, siderite, feldspar, and mica (Grimshaw, 1971, pp.29–37). Fe hydroxides (often Fe3+ forms) are frequently precipitated or adsorbed on kaolin surfaces or admixed as a distinct phase, leaving much of the kaolin unsuitable for commercial use due to inadequate whiteness or loss of certain refractory qualities (ŠTYRIAKOVÁ and ŠTYRIAK, 2000). The amount of Fe (III) impurities in kaolin affects the quality of kaolin.

The refining of low-grade clay is a required resource for the production of high-grade clay. Various physical, chemical, and microbiological procedures have been implemented to remove the ferric Fe contained in kaolin as oxide or hydrated oxide (LEE, CHO and WOOKRYU, 2002). One of the chemical methods is using the strong reducing agent, sodium dithionite can remove the bulk of the Fe and leave low pure white kaolin at low pH but they work under extreme conditions and are costly (Conley and Lloyd, 1970). According to Arslan and Bayat (2009), the removal rate of iron from kaolin was 94.89% under ANOVA-Yates test techniques of the chemical leaching test. Its whiteness index can be reached up to 90.60 %. Its optimum chemical leaching conditions were under 80 $°C$, 0.2M concentration of the oxalic acid, and 15% w/v of pulp density within 120 minutes. The using of commercial organic acids such as oxalic acid and citric acid also belongs to the chemical leaching method (Musial, Cibis and Rymowicz, 2011).

The bio-hydrometallurgical process is highly efficient and is less detrimental to the environment than conventional processes (Musial, Cibis and Rymowicz, 2011; Hosseini and Ahmadi, 2015). Bioleaching is a sustainable and environmentally friendly approach to extracting valuable metals from ores and minerals (Admin, 2021). This process utilizes microorganisms to solubilize metals from solid substrates through various mechanisms (HALVORSON and

STARKEY, 1927, pp.381–402). *Bacillus.* sp require iron to conduct the metabolic process in the destruction of silicate minerals (Štyriaková et al., 2003). Fe (III) cannot be reduced abiotically in the absence of glucose, in sterile glucose-containing media and low pH during incubation with the *Bacillus.* sp (Koloušek et al., 2007). Oxalic acid is mostly produced by the fungus *Aspergillus niger* in terms of the microbial of interest (Musial, Cibis and Rymowicz, 2011).

In recent years, there has been a growing interest in optimizing bioleaching processes by exploring surface, chemical, and structural studies. This literature review aims to provide an overview of the key aspects related to the optimization of bioleaching, focusing on the bioleaching of kaolin as a case study. The discussions are about the effects of bioleaching, techniques employed, factors influencing the process, ways to enhance it, microbial iron reduction, adhesion mechanisms, and the findings in this field.

2.2 Bioleaching of Kaolin

Bioleaching of kaolin involves the use of microorganisms to extract metals and impurities from the mineral through their metabolites (Hosseini and Ahmadi, 2015). *Bacillus* sp. bacteria can reduce the amount of free Fe as well as Fe bound in mica, which frequently contaminates kaolins (ŠTYRIAKOVÁ and ŠTYRIAK, 2000).

The application of bioleaching to kaolin processing has the advantage of reducing the environmental impact associated with traditional methods (Mesquita, Rodrigues and Gomès, 1996; ŠTYRIAKOVÁ and ŠTYRIAK, 2000). It is because it uses naturally occurring microbe to facilitate the process and can reduce the need for harsh chemicals such as sulphate oxide (Koloušek et al., 2007).

Bioleaching is more selective, it allows for the targeted extraction of specific metals from complex mineral ores. With the proper conditions such as a related microbe, sample and medium, the specific metals can be targeted. The mixture of *Bacillus* strains extracted 39% Si, 60% Pb, 43% Zn and 32% Cu from flotation concentrate, 33% Si, 75% Pb, 76% Zn, 76% Cu and 82% Mn from post-flotation waste, 30% Si, 59% Pb, 35% Zn, 56% Cu, 78% Mn, 37% A1 and even 30 % Au from gravitational concentrate (Štyriaková, Štyriak and

Kušnierová, 1999). The samples obtained from different methods and locations will extract different percentages of mineral content by bioleaching. The most targeted metal in kaolin is iron, because the whiteness index will be influenced and become impurities (Tracy, 2018).

2.3 Effect of Bioleaching

Bioleaching has a profound effect on the composition and structure of kaolin. It alters the mineral's chemical composition and reduces impurities, making it suitable for various industrial applications. Additionally, bioleaching can significantly increase the recovery of valuable metals present in kaolin. Table 2.1 shows the types of microorganisms, a related condition, result and their reference. The results were focused on collecting the reduction rate of Fe and the whiteness index improvement within the year from 1995 to 2023. The microorganisms belong to fungi and bacteria. The techniques of bioleaching were the in-situ method and the two-stage bioleaching method.

From Table 2.1, the highest whiteness index under bioleaching of fungi (*A.niger*) was 81.1% and the highest removal rate of iron was 77.13%(Arslan and Bayat, 2009). For the bioleaching of bacteria (Fe (III)-reducing bacterial consortia), the achievement of the highest whiteness index was 81.5 % (Guo et al., 2010b). *B. cereus* had the most efficiency in reducing iron containment in the nitrogen-rich medium, it was close to 80 % (Jing et al., 2021).

The microbial reduction of Fe impurities in kaolin clay results in considerable changes in mineral surfaces, as seen by the morphology of bioleaching. Štyriaková et al. (2003) reported that *Bacillus* sp. bioleaching caused the mica, a hardy mineral found in kaolin, to lose its tetrahedral and octahedral units. The primary cause of these morphological alterations is thought to be bacterial metabolite synthesis, especially the creation of organic acids, which remove Fe (III) and aid in the deterioration of mineral surfaces.

According to Guo et al. (2010a), XRD analysis was conducted after bacterial treatment of kaolin, which revealed slight structural changes and a growth in crystallinity but no significant development of secondary mineral phases. Zegeye et al. (2013) employed SEM to observe untreated kaolin with well-crystallized and hexagonal particles, while bacteria-treated samples exhibited rounded particles with slightly damaged edges.

Figure 2.1 shows the SEM image of the untreated kaolin and treated kaolin with *B.cereus* strain UKMTAR-4 (Yap et al., 2020). The highlighted part for the Figure 2.1 a was rounded edges and amorphous structure while for the Figure 2.1 b was sharp edges and crystalline structure. These findings aligned with the results of Yap et al. (2020), who reported a transition from a more amorphous to a more crystalline structure in untreated mineral surfaces after contact with bacteria, corroborating Zegeye et al.'s observations.

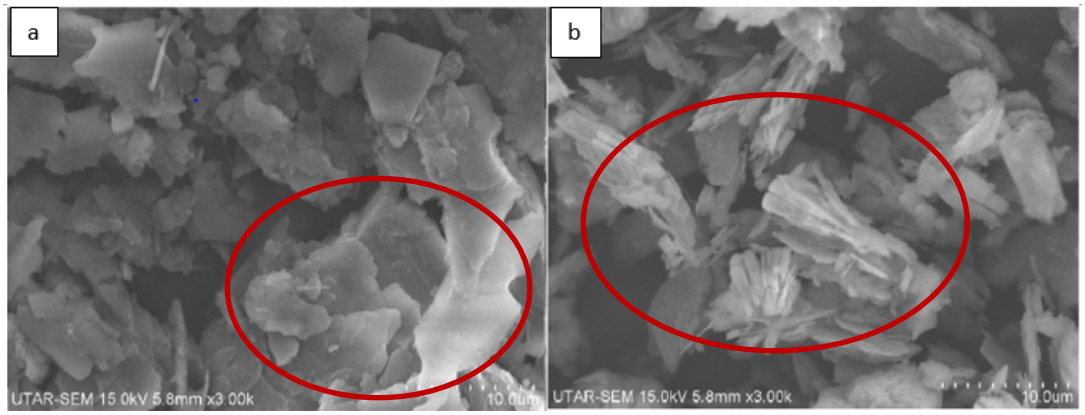

Figure 2.1: a) SEM image of the untreated kaolin. b) SEM image of the treated kaolin with *B.cereus* strain UKMTAR-4 (Yap et al., 2020).

In summary, the observation of surface morphology during bioleaching demonstrates that microbial processes can induce notable changes, although the extent and nature of these changes may vary.

2.4 Technique of Bioleaching (in situ & two-state bioleaching methods)

There are two primary methods for bioleaching in the context of kaolin: in-situ bioleaching and two-stage bioleaching. In-situ bioleaching, also known as in-place bioleaching, is a method where microbial activity takes place directly within the kaolin deposit. It is simple because it allows the selected microorganisms to grow and bioleach the target metals in their natural environment by involving carbon sources directly in the mineral deposit. This method is typically used for low-grade or bulk kaolin deposits where it is not economical to mine and process the material conventionally. Due to the minimizing of the need for extensive mining and ore processing operations, in-situ bioleaching can be a cost-effective and environmentally friendly way to recover valuable metals or improve the quality of kaolin (Cameselle et al., 2003).

Some of the limitations to obtaining the optimum operating conditions by in situ bioleaching are different. The efficiency of the bioleaching will be limited by microbial metabolism and growth constraints. Different type of minerals has their different optimum condition for pH, temperature, and nutrients.

Two-stage bioleaching involves two separate steps or stages in the bioleaching process (Groudev, 1987). In the first stage, the kaolin ore is typically mined and crushed to expose the minerals of interest. The crushed ore is then subjected to bioleaching in a separate reactor or tank, where microorganisms are introduced to dissolve the minerals. This method is often used for higher-grade kaolin deposits or when specific minerals within the kaolin need to be targeted for extraction. Two-stage bioleaching allows for better control over the bioleaching conditions and the extraction process.

According to Musial, Cibis and Rymowicz (2011), fungal biomass growth and organic acid synthesis by *A. niger* occur in the bioreactor under optimal conditions as the first step. The fermented medium containing oxalic acid after the separation of biomass can be immediately used as a bleaching agent for the second step. As a consequence, two-stage bioleaching can eliminate the drawbacks of in-situ bioleaching. This is because kaolin can hinder biomass growth and oxalic acid synthesis in microbial processes. Recovering kaolin from biomass presents substantial challenges due to its integration into the biological matrix, requiring specialized separation methods. Furthermore, maintaining sterility in both kaolin and the culture medium is paramount for microbiological and biotechnological processes to prevent contamination and ensure culture purity.

In summary, the main difference between in-situ and two-stage bioleaching for kaolin lies in the location and approach to microbial activity. In-situ bioleaching occurs within the deposit itself, while two-stage bioleaching involves a separate processing step after mining. The choice between these methods depends on factors such as the quality of the kaolin deposit, the specific minerals or metals of interest, and economic considerations. According to Cameselle et al. (2003), the whiteness index was improved from 56.5% to 80% within 40 hours through the two-stage bioleaching process or else it took 10 days to achieve the same improvement rate by in situ method. As a result, the

two-stage process is preferable to obtain high-quality kaolin (Musial, Cibis and Rymowicz, 2011).

2.5 Factors Affecting Bioleaching

Figure 2.2 shows the result in the observation time slot of 28 days. It involved two types of fungi (*A. niger* isolated from pistachio shell and NCIM 548), at two different temperatures (25 °C and 30 °C). The first pill was the brightness in observation, which was in the condition of *A. niger* isolated from a pistachio shell at 25 °C. The second pill was in the condition of *A. niger* isolated from pistachio shell at 30 °C. The third pill was in the condition of *A. niger* NCIM 548 without cells at 25 °C. The fourth pill was in the condition of *A. niger* NCIM 548 without cells at 30 °C. The fifth pill was in the condition of *A. niger* NCIM 548 with cells at 25 °C. The sixth pill was in the condition of *A. niger* NCIM 548 with cells at 30 °C. The last pill was the primary kaolin sample without any control.

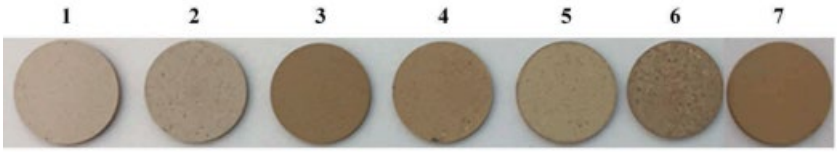

Figure 2.2: Diagram of the pills prepared from kaolin powders after 28 days (Hajihoseini and Fakharpour, 2019).

Several factors influence the efficiency of bioleaching, including the type of microbe, pulp density, concentration of medium, pH, temperature and duration. From Figure 2.2, the whiteness index was influenced by the type, the presence or absence of cells and the temperature. These conditions will contribute to the bioleaching process through metabolic activities. The difference between the untreated sample and the bioleached samples can be obviously observed from the improvement of the brightness. Thus, understanding and optimizing these factors are crucial for enhancing the bioleaching process.

2.5.1 Type of microbe (Fungi and Bacteria)

Microorganisms play a vital role in reducing impurities present in kaolin. Certain bacteria can mediate the reduction of iron impurities, which not only improves the quality of kaolin but also releases valuable metals for recovery. They can affect the efficiency of the iron removal rate.

According to Hosseini et al. (2007), *A. niger* isolated from pistachio shell and *A. niger NCIM 548* were used. The iron removal rate from *A.niger* from pistachio shell was 42.8% and *A. niger NCIM 548* was 2.2% even though the condition of pulp density and the time observation were the same. *A. niger NCIM 548* still resulted in approximately 20 times lower than the strain isolated from the pistachio shell. They produced different contents of organic acid and caused the difference in iron dissolution.

In the pH range of 6 and 7, *A.niger* produced oxalic acid from saccharides (Bohlmann et al., 1998). The generated acid was citric acid when the pH was lower under biosynthesis (Santoro et al., 1999). *A. niger* produced a large amount of oxalic acid in the lipid-enriched medium under the range of pH between 4 to 5 (Rymowicz, 2003). Oxalic acid was the most efficient by comparing the various organic acids as leachants. According to Musial, Cibis and Rymowicz (2011), oxalic acid is mostly produced by the fungus *A. niger* under the optimum condition of pH and the composition of the production medium. It was less efficient for the iron removal rate. In contrast, it had higher efficiency for copper, zinc, and nickel removal.

Fungi play a vital role in leaching processes by excreting organic acids and creating an acidic environment to greatly dissolve the metal compounds through processes such as protonation, complexation, and reduction (Hosseini and Ahmadi, 2015). Particularly, it can be used for the removal of iron impurities from kaolinite clays. *A. niger* is often preferred for its efficiency in producing oxalic acid, which is a key component in these bioleaching processes (Hosseini et al., 2007).

As part of natural and contaminant biogeochemical cycles, microorganisms play a crucial role in removing iron oxide/hydroxide from kaolinite clays (Kostka et al., 2002). According to BROMFIELD (1954), the iron-reducing bacteria were unable to utilize ferric oxide as a source of oxygen for their growth under anaerobic conditions. Instead, they required an external

compound containing available oxygen to support their growth and facilitate the reduction of ferric compounds. This finding highlights the specific environmental requirements of these bacteria.

Under anaerobic conditions, microorganisms can reduce Fe III in kaolin, even in structural forms, for purposes other than iron assimilation, generating soluble Fe II that can be removed (Lee et al., 1999; Štyriaková et al., 2012; Zegeye et al., 2013). These microbes use organic compounds or hydrogen such as sugars, amino acids, mono-aromatic compounds, and long-chain fatty acids as electron donors, with Fe III serving as the sole electron acceptor (Zegeye et al., 2013).

Contrary to previous assumptions about the reactivity of Fe III based on crystallinity, later studies have shown that the amount of Fe III reduction is more influenced by iron oxide's surface area than by its crystallinity (Kostka et al., 2002). While structural Fe III impurities in kaolin are less bio-available and little reduced, they are more receptive to reduction in other clay minerals such as smectite, nontronite, chlorite, and illite. (Zegeye et al., 2013).

Kostka et al. (2002) conducted comparative research using Shewanella species, demonstrating the reduction of structural Fe III and suggesting temperature as a crucial factor. Štyriaková and Štyriak (2000) found that *B. cereus* strains removed free iron and some iron bound in mica. They also observed the mica structure was gradually being destroyed and that illite was forming. Moreover, Zegeye et al. (2013) reported minimal structural modification during bioleaching.

By acting as electron shuttles or increasing the availability of iron for reduction, ligands and chelators in the growth medium can hasten iron dissolution. Oxalate, an organic ligand, may promote the process by acting as a carbon source. (Kostka et al., 2002).

2.5.2 Pulp density

According to Hosseini et al. (2007), higher pulp density made a higher iron dissolution rate because of the addition of the higher amount of kaolin in Figure 2.3. The raising of pulp density increases the contact surface between the solid phase and microorganisms under the assumption that particle size is constant,

and it accelerates the dissolution. Iron concentration increased while the sugar concentration decreased and pH decreased accordingly.

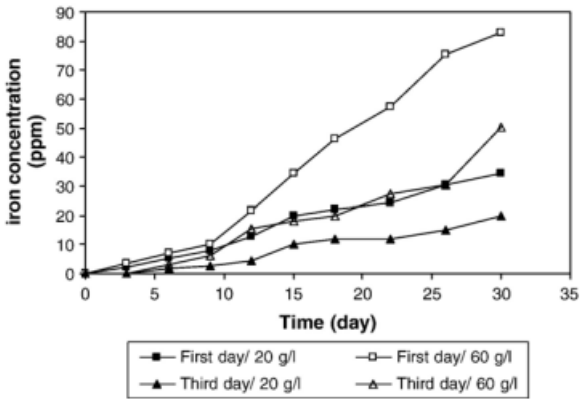

Figure 2.3: Iron removal rate during bioleaching experiments (Hosseini et al., 2007).

According to Arslan and Bayat (2009), Bioleaching tests using *A. niger* at 1.5% w/v showed that increasing the pulp density adversely influenced the removal of Fe in Figure 2.4. Under the optimum pulp density, the highest rates of dissolution were achieved at the beginning of the experiment, followed by a reduction in the removal rate of Fe dissolved until it obtained the maximum Fe concentration.

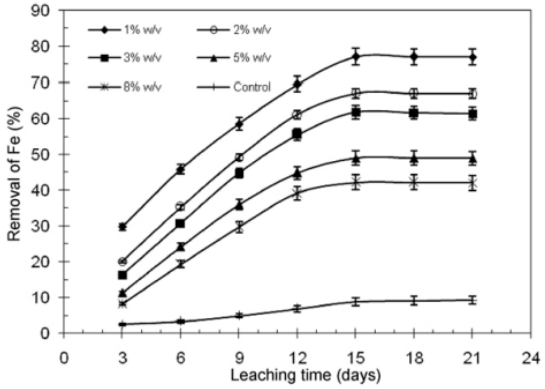

Figure 2.4: Removal of Fe during bioleaching experiments (Arslan and Bayat, 2009).

Pulp density adjustments did not negatively impact iron removal in clay due to its low organic content which eliminated their inhibitory effect (Cameselle et al., 2003; Hosseini et al., 2007; Arslan and Bayat, 2009).

2.5.3 Concentration of medium

Microorganisms involved in bioleaching require specific nutrients to thrive and carry out metal solubilization. These nutrients typically include carbon sources (such as sugars or organic acids), nitrogen sources (such as ammonium ions or nitrates), and other essential minerals (Cameselle et al., 2003; Štyriaková et al., 2003; Musial, Cibis and Rymowicz, 2011). The concentration of these nutrients in the medium should be optimal for the microorganisms to grow and efficiently leach metals. Too low a concentration can lead to slow microbial growth and reduced metal solubilization, while too high a concentration may not provide any additional benefits and can be wasteful or detrimental to the microorganisms.

Furthermore, the choice of carbon and nitrogen sources can impact iron removal rates, with monosaccharides being more efficient and $(NH_4)_2SO_4$, serving as an effective nitrogen source (Lee et al., 2002; Guo et al., 2010a). Glucose is an efficient source of carbon and energy for heterotrophic bacteria. Fe reduction greatly increased when glucose was involved due to the microbial production of acids by *B.cereus* (Štyriaková et al., 2003). The fermentation time of bacteria was influenced by the concentration of glucose as shown in figure 2.5.

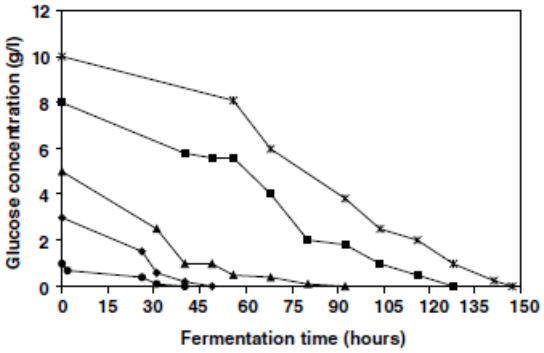

Figure 2.5: Glucose consumption during bioleaching of kaolin measured by on-line method (Nandakumar et al., 1999).

According to Hosseini et al. (2007), the sugar concentration decreased from 120g/l to 68.5g/l when the iron removal occurred with the bioleaching of *A.niger*. To build the economically competitive oxalic acid in the biosynthesis of *A.niger*, it can grow in the cost renewable carbon feedstocks such as beet

molasses, green corn syrup, and sweet potato from agriculture or industry (Musial, Cibis and Rymowicz, 2011). In addition to the carbon source, the medium for oxalic acid production must be enhanced with adequate levels of nitrogen, phosphorus, and magnesium. According to Musial, Cibis and Rymowicz (2011), it demonstrated the potential of using biodiesel-derived waste as a substrate for oxalic acid production by *A. niger* XP, highlighting the strain's ability to efficiently utilize glycerol and free fatty acids simultaneously, which can lead to higher yields of oxalic acid.

The choice of carbon and nitrogen sources plays a crucial role in influencing the pH and bioleaching efficiency during iron removal from kaolin using bacteria. Studies by Guo et al. (2010a) revealed that monosaccharide carbon sources like glucose were more efficient for iron removal compared to disaccharides and polysaccharides, likely due to their direct utilization as electron donors by the bacteria. Regarding nitrogen sources, the addition of $(NH_4)_2SO_4$, beef extract, and $CO(NH_2)_2$ enhanced iron dissolution, with $(NH_4)_2SO_4$ being the most effective. Notably, $(NH_4)_2SO_4$ not only increased iron dissolution but also accelerated the bioleaching rate, reducing the required incubation time to reach maximum iron removal.

Interestingly, Jing et al. (2021) proposed that the Gram-positive bacteria *Bacillus cereus* and *Staphylococcus aureus* facilitate iron reduction by basifying the medium, in contrast to some Gram-negative bacteria like *Pseudomonas* and *Shewanella oneidensis*, which acidify the surrounding medium through organic acid production. For *B. cereus*, ammonia production in nitrogen-rich media increased the pH above 8.5, promoting bacterial adhesion to ferric oxide surfaces. Siderophores like ferrioxamine B/desferrioxamine B and petrobactin shuttled ferric ions into bacterial cells, where they were reduced to ferrous state by cellular reductases and the alkaline environment. Similarly, *S. aureus* adhered to amorphous ferric ions on kaolin, with the iron-regulated surface determinant (Isd) system facilitating ferric ion binding and internalization. The siderophore staphyloferrin bound ferric ions, which were reduced to a ferrous state by the iron uptake oxidoreductase (IruO). Basification also upregulated genes like sigB and DacA, promoting ammonium/glutamine uptake and ferric reduction for pH homeostasis. The basification of the medium is hypothesized to promote

bacterial adhesion to the iron oxide surface and trigger cellular mechanisms for ferric ion reduction by these Gram-positive bacteria.

Lee et al. (2023) observed significant pH changes during bioleaching experiments with Bacillus species (*B. cereus, B. aryabhattai, and B. megaterium*) in the presence of glucose. Within the first two days, the pH dropped sharply from around 4.5-4.6 to 2.8-2.9, followed by a steadier but slower decrease, reaching around 2.5 by day 10. This decreasing pH trend was consistent across the different Bacillus species, suggesting the production of organic acids, which likely played a role in iron dissolution from the kaolin.

In summary, the use of different carbon and nitrogen sources, such as glucose and $(NH_4)_2SO_4$, respectively, can enhance iron removal and bioleaching efficiency. Additionally, the pH changes observed during bioleaching with Bacillus sp. suggest the production of organic acids, which likely play a role in iron dissolution from the kaolin.

2.5.4 pH value

The bacterial activity is affected by the pH value. An appropriate pH of the culture medium can enhance the activities of microbes in bioleaching. The solubilization of metals and the stability of metal ions were influenced in the liquid phase. When the pH value was lower than 5, the bacterial activity was terminated although involving glucose (Štyriaková et al., 2003). The pH value was influenced by the release of acid from the iron reduction under bioleaching. The releasing of organic acids was oxalic acid, citric acid and gluconic acid (Cameselle et al., 2003).

Cell development produces a drop in nitrogen concentration during the initial hours of incubation. When nitrogen is reduced, organic acid production increases ((Musial, Cibis and Rymowicz, 2011). The production of oxalic acid was generated with the advancement of the time observation, pH value was gradually decreased until it reached its saturation point. Due to the low pH in the medium, bioleaching is generally considered a combination of bioleaching and chemical leaching (Fonti, Dell'Anno and Beolchini, 2016).

2.5.5 Temperature

According to Table 2.1, the main reference temperature selected to investigate the microbe activity was 30 ºC. Two-stage bioleaching has proven to be a valuable approach for conducting processes at elevated temperatures, which would otherwise be unfavourable for microorganisms in an in-situ setting. Cameselle et al. (2003) employed a full factorial design to investigate this method.

The researchers had previously experimented with two-stage bioleaching using the spent fermentation substance of *A. niger* CBS 246-65 at higher temperatures to explore the potential for improving iron dissolution (Cameselle et al., 1995). Their comprehensive study examined various factors including changes in pH value, temperature and citric acid concentration. The outcomes were noteworthy, with a substantial 43% removal of iron oxide impurities achieved at 60 °C after just 5 hours, resulting in a significant improvement in the whiteness index to 67%. Importantly, the absence of enzyme activity at these elevated temperatures led to the conclusion that extracellular enzymes had little to no impact on iron solubility and that organic acids predominantly assisted it.

Furthermore, Arslan and Bayat (2009) conducted a comparison of kaolin produced by chemical leaching with kaolin from a bioleaching process utilizing A. niger. The maximum iron reduction, 95% was achieved using the chemical method at a temperature of 80 °C and a pulp density of 15% w/v. In contrast, the bioleaching experiments yielded remarkable results under milder conditions, achieving the reduction of 77.13% of total iron at a pulp density of only 1% w/v, under 25 °C, a spore concentration of 3×10^7 spores/l, and a particle size below 63 mm after 3 weeks. These findings are consistent with previous reports (Cameselle et al., 2003; Hosseini et al., 2007).

Additionally, Musial, Cibis and Rymowicz (2011) demonstrated that the whiteness index of kaolin could be significantly enhanced to 79.4%. This achievement was accomplished by employing a kaolin content of 20 g/l, a solution consisting of 27.5 g/l oxalic acid, and a rising temperature of 50 °C, all within a relatively short duration of 1.7 hours. In conclusion, these studies use the potential of two-stage bioleaching as an effective method for mineral

processing at high temperatures, offering valuable insights into optimizing iron removal and improving material quality.

2.5.6 Duration

From Table 2.1, the time consumption for two-state bioleaching is lower than the in-situ method. According to Cameselle et al. (2003), the result of the iron removal rate was the same with the in-situ method and two-state method but the time taken for the in-situ method was 10 days while the two-state method was 40 hours. The duration can be shortened with the correct technique of bioleaching. According to Hosseini et al. (2007), the effect of time of clay addition was not significant when compared to the interaction between strain and pulp density from the statistical model. It was because they had reached their saturation point to react.

2.6 Ways to Enhance the Bioleaching Process

Enhancing bioleaching involves strategies such as optimizing nutrient availability, controlling environmental conditions, and selecting or engineering microorganisms with enhanced metal solubilization capabilities. The microorganism selection is important as section 2.5.1 mentioned because the ability of microorganisms to purify the kaolin is different. The cultured environment of microorganisms from section 2.5 is the factor which will directly affect the efficiency of the iron removal rate and the improvement of the whiteness index.

Table 2.1 shows the final results that were investigated by the following researchers. They show the optimal conditions to obtain the best efficiency of iron removal rate and whiteness index by controlling the factors, such as types of microorganisms, temperature, concentration of medium, pulp density, time observation and technique of bioleaching. These approaches can improve the efficiency and yield of bioleaching processes.

2.7 Inconsistency of Iron Reduction Mechanism

While microbial iron reduction is a promising aspect of bioleaching, there is still inconsistency in understanding the exact mechanisms involved. The mechanisms of Fe (III) reduction in clay ore can vary depending on factors such

as the type of clay mineral, the extent of reduction, and the presence of organic matter in the agent (Yong et al., 2022).

The different types of clay minerals in different places contain different structures and components. They are decided from the weathering and transformation in soil, the influence of the pH on the environment, and the impact of the reduction of structural iron (Hosseini and Ahmadi, 2015). The reduction of structural iron has several consequences, including alterations in swelling behaviour, colouration, specific surface area, cation exchange capacity, and magnetic interactions. Additionally, it leads to the compaction of clay layers and the entrapment of cations within the mineral matrix, rendering essential nutrients inaccessible for agricultural use.

If the extent of dissolution is small, infrared spectroscopy makes it hard to detect the dissolution product. The organic matter with produces hydrogen ions will reduce Fe (III) and acidify the medium to enhance the kaolin dissolution (Yong et al., 2022). Further research is needed to elucidate the microbial processes responsible for iron reduction in kaolin bioleaching.

2.8 Primary Adhesion of Bacteria

The primary adhesion of microorganisms to the kaolin surface is a critical step in bioleaching. According to Štyriaková, Štyriak and Kušnierová (1999), the primary adhesion involves the important role of bacteria, especially for the genus *Bacillus*. They were significant in the initial stages of mineral weathering and destruction. With the adhesion of minerals on the surface, the involved bacteria facilitated their breakdown potentially. It is considered a form of primary adhesion as it involves the initial interaction of bacteria with mineral surfaces.

The electrostatic and hydrophobic interactions are detected in the primary adhesion of microorganisms (Yong et al., 2022). It relies on the balance of the attractive and repulsive force between the microorganism cell and mineral surfaces. Electrical forces arising from electrical double layers and the attractive Van der Waals interactions between the sticky particles, collectively known as DLVO forces, play a role in bacterial adhesion (Tsuneda et al., 2003). Additionally, polymeric interactions, especially in cases with a significant amount of extracellular polymeric substances (EPS), contribute to adhesion.

Bacterial cell surface hydrophobicity is important; hydrophobic cells are more likely to adhere to mineral surfaces, as they are less affected by electrostatic repulsion from water molecules.

2.9 Second Stage Adhesion of Bacteria

After the initial attachment, microorganisms undergo a second stage of adhesion, forming biofilms on the kaolin surface. Studying the factors influencing this stage can lead to better control of microbial activity and enhanced bioleaching efficiency.

According to Štyriaková, Štyriak and Kušnierová (1999), the secondary adhesion involved the isomorphic substitutions, formation of authigenic minerals, extraction of iron from kaolin and the function of *Thiobacillus* Bacteria. The isomorphic substitutions of silicon for aluminium in the mineral structure weaken the resistance of the structure. These elements are extracted into solution and subsequently transformed by bacterial sorption into new secondary clay minerals, possibly aluminosilicates of allophanic composition.

Bacillus species, such as *Bacillus subtilis*, have been implicated in the development and growth of authigenic (made in situ) minerals such as allophane and imogolite. This is also a type of secondary adhesion since it includes the joining of mineral components to produce new mineral structures in the presence of bacteria. The extraction of iron from kaolin makes the formation of high-quality kaolin under natural conditions. It involved the transformation and adhesion of elements in the medium by bacteria. *Thiobacillus* bacteria perform the destruction of sulphides released from non-ore matrices on the mineral surface after primary weathering.

The secondary adhesion encompasses processes where bacteria facilitate the transformation, binding, or recombination of mineral components after the initial stages of weathering have occurred. It represents a critical stage in the complex interplay between bacteria and mineralogical processes within geological environments (Štyriaková, Štyriak and Kušnierová, 1999). The second stage of microbe-mineral interaction involves irreversible attachment facilitated by EPS, leading to biofilm formation (Yong et al., 2022). EPS is a complicated compound of biopolymers like nucleic acids, polysaccharides,

lipids, and proteins. It can contribute to the formation of clay-rich soils, the development of clay minerals like kaolinite or smectite, and the creation of stable mineral aggregates.

2.10 Summary

In summary, the optimization of bioleaching using surface, chemical, and structural studies is a promising avenue for extracting metals from kaolin and other minerals efficiently and sustainably (Musial, Cibis and Rymowicz, 2011; Hosseini and Ahmadi, 2015). Factors affecting bioleaching, techniques employed, and the role of microorganisms in iron reduction are key areas of research. Further investigation is required to fully understand microbial leaching in natural systems to explore the role of the inoculum and organic matter in iron reduction, and the role of electrostatic charge and hydrogen bonds in the primary and secondary adhesion of bacteria (Yong et al., 2022).

Previous studies have highlighted the significant issue of bioleaching duration, which has hindered the widespread industrial adoption of biotreatment methods. The metabolic processes of bacteria involved in bioleaching typically span a duration ranging from 5 to 90 days, posing a considerable challenge. Despite its sustainability and potential to achieve comparable iron removal rates to conventional methods, the time-intensive nature of bioleaching remains a deterrent. However, the primary focus of business stakeholders tends to prioritize company profits. As researchers, our focus lies in identifying optimization factors aimed at enhancing efficiency and shortening reaction durations within bioleaching processes.

Table 2.1: Summary table of the studies of bioleaching in kaolin.

Microbe	**Condition**	**Result**	**Reference**
A. niger CBS246-65	- 15g kaolin - 30°C - 200rpm - Two-stage bioleaching	- 43% of iron removal rate. - The whiteness index improvement was raised from 56.5% to 67%.	(Cameselle et al., 1995)
B. cereus strain	- 10g kaolin sample - 100 ml amended Bromfield medium - Anaerobic condition - 1 to 3 months - 28 °C	- 43% of iron removal rate for 1-month bioleaching. - 52% of iron removal rate for 3 months of bioleaching. - In SEM observation, the mica surface was destroyed when Fe ions were released from the mica structure.	(ŠTYRIAKOVÁ and ŠTYRIAK, 2000)
Iron removing bacteria	- 10g kaolin - 50 ml mixture culture - 30°C - In situ method	- Removal of Fe from 3.22mg to 1.35mg in 5% of maltose (58% of improvement). - The whiteness index was increased from 64.49 to 71.5%. - Fe impurities were removed without changing the mineralogical composition of kaolin under bioleaching.	(LEE, CHO and WOOKRYU, 2002)

fungus *A. niger* CBS 1120	- sucrose inoculum supplemented with NH_4NO_3 and KH_2PO_4 - 30°C - pH 6 - 15g kaolin	- A large amount of oxalic acid was produced for iron removal in the first stage of active metabolism production. - *A. niger* on kaolin, the efficiency is largely dependent on the strain used. After two-stage bioleaching, - 100% of iron removal was obtained in 40 hours at pH 2. - An 80% whiteness index was obtained.	(Cameselle et al., 2003)
B. cereus strain	- Bromfield medium (100ml) - kaolin (10g) - 3 months - 30 °C	- 49% of iron removal rate. - No bacterial activity occurred when pH < 5	(Štyriaková et al., 2003)
A. niger (indigenous isolate from pistachio shell and NCIM 548)	- kaolin (2-6 g) - Culture media (100 ml) inoculated with 10^6 spores/mL - 30 days - 30 °C	- Bioleaching with *A. niger* (pistachio shell) resulted in greater iron removal efficiency in clay at 42.8%, while *A. niger* NCIM 548 only managed a 2.2% removal rate with the	(Hosseini et al., 2007)

	- 160 rpm - In situ method	same pulp density of 20g/l.	
A. niger	- Different pulp densities (1–8% *w*/*v* solid concentration) - 150 mL medium - 3 weeks - 30°C -150 rpm - In situ method	- The removal of Fe was restricted by increasing pulp density. - At 1% w/v pulp density at 25 °C and its pH value was 1.5 at day 21, the largest iron reduction rate was reached, 77.13%. - Whiteness index of bioleached kaolin was 81.1%.	(Arslan and Bayat, 2009)
Fe (III)-reducing bacterial consortia	- 10 g of kaolin - 100 ml of distilled water - 1 g of carbon source and 5 ml of blended culture broth - 30 °C - 10 days - In situ method	- Fe removal efficiencies were affected by the different carbon sources with the following sequences of monosaccharide, disaccharide, and polysaccharide. - 51% of the iron removal rate was reached and the improvement of the whiteness index was raised from 61% to 82% with the	(Guo et al., 2010a)

		involvement of 5% of food sugar. - The secondary mineral phase and structural changes did not occur but its crystallinity was improved under bioleaching.	
Fe (III)-reducing bacterial consortia	- 10 g of kaolin - 100 ml of glucose medium, and 5ml of mixed culture broth, - 30 °C - 10 days - In situ method	- Whiteness index improvement was increased from 60.8% (untreated without firing) to 81.5% (treated without firing) and 83.8% (untreated with firing) to 92% (treated with firing). - The optimum pH range was 4.6 to 6.0, the optimum incubation temperature was 35 °C, the optimum pulp density was 10%, and the optimum inoculum density was 30%.	(Guo et al., 2010b)
A. niger XP (*A. niger* pistachios and NCIM 548 *A. niger*)	- Oxalic acid production through immersed batch culture utilizing	- The brightness index was advanced from 74% to 79.2% in kaolin. - 13.7% of iron removal rate.	(Musial, Cibis and Rymowicz, 2011)

	biodiesel-derived waste (pH 4.5, 500 rpm, 30 °C) - 600 mL oxalic acid-enriched fermented medium (sulfuric acid, pH 3), 100 rpm was used for bioleaching of kaolin - Two-stage bioleaching	- The optimal temperature is 49.12°C and takes 1.668 hours.	
Shewanella alga BrY, *S. putrefaciens* CIP8040, *S. putrefaciens* CN32, *S. oneidensis* MR-1	- Medium containing 10 mM of sodium methanoate as the electron donor - 10 or 20 g of kaolin as the final electron acceptor - 0.9% of NaCl and 100 µM AQDS. - 20 or 30 °C - darkness	- Kaolin ferric iron was reduced and leached by all bacterial strains. - *S. putrefaciens* CIP8040 provided the highest increase in ISO brightness (74% to 79%) and whiteness index (54% to 66%). - The kaolinite did not show any secondary mineral or crystal-chemical alteration. - The original hexagonal shape of the clay particles became	(Zegeye et al., 2013)

	- 5 days - 320 rpm - In situ method	stochastic under bioleaching.	
A. niger (indigenous isolate from pistachio shell and NCIM 548)	- Injection of culture medium (100ml) with fungus and kaolin (5g) - 28 days - 25 °C & 30 °C -160 rpm	- For *A. niger* (pistachio shell), the iron removal rate was 47.7% at 25 °C after 14 days, it was greater than at a temperature of 30 °C, which was 33.8% after 28 days. - The whiteness index improvements in bioleached samples were 74.49% at 25 °C and 75.41% at 30°C, while the untreated kaolin was 71.94% for *A. niger* NCIM 548.	(Hajihoseini and Fakharpour, 2019)
B. cereus (procured commercially and UKMTAR-4)	- 80 mL glucose solution (bioleaching occurred) - kaolin (10g) - 5 to 10 days - 250 rpm - 30 ◦C - two-stage bioleaching	- *B. cereus* UKMTAR-4 could remove 53.9% of Fe, which was higher than *B. cereus* (33.9%). - Compared to untreated kaolin, the surface of biotreated kaolin showed some damage and a little cracked structure. - The bacteria concentration was	(Yap et al., 2020)

		proportional to the bioleaching activity.	
B. cereus UKMTAR-4, *Burkholderia thailandensis* MSMB43, *Escherichia coli* K-12, *Pseudomonas aeruginosa DWW3, Staphylococcus aureus* NCTC 6571	- 50 mL of nitrogen-rich medium - 1 g kaolin powder - 14 days - 160 rpm - room temperature	- Efficiency of Fe removal rate followed by the highest, *S. aureus* (76.2%), the second highest, *B. cereus* (38.7%) and *B. thailandensis* (31.4%) - The whiteness index of the biotreated sample was improved when compared to the untreated kaolin. - *P. aeruginosa* and *E. coli* showed no change obviously in the ferrous level by no changing of pH values - Under further investigation, *B.cereus* was the most efficient in reducing iron containment in a nitrogen-rich medium, it was close to 80% compared to *S. aureus* (30%)	(Jing et al., 2021)
Bacillus sp. (*B. cereus* UKMCC 1150, *B. aryabhattai* UKMCC 1151	- 20g kaolin - 200ml of 10g/L glucose solution - 10 days	-*B. aryabhatti* had the highest removal efficiency of Fe, 65.3%, *B.megaterium*	(Lee et al., 2023)

& *B. megaterium* UKMCC 1152)	- 30°C	(56.2%) and *B. cereus* (47.7%) -*B. megaterium* had the highest whiteness index improvement of 13.6%, *B. aryabhattai* (7.4%), and *B.cereus* (6.6%) -Glucose concentration decreased progressively under bioleaching, where *B.cereus* consumed from 9.5 to 8.2 g/L - pH changed significantly in the first two days under *B.megaterium* from pH 4.6 to 2.8	

CHAPTER 3

METHODOLOGY AND WORK PLAN

3.1 Introduction

Figure 3.1 shows the methodology of bioleaching. It involves preparations of kaolin and inoculum, bioleaching of kaolin, and techniques analysis for chemical, surface, and structure. 1-10 phenanthroline colourimetric methods and energy dispersive X-ray (EDS) are under chemical analysis. Scanning Electron Microscopy (SEM) belongs to surface analysis. The structure analysis includes X-ray diffraction (XRD) and Fourier Transform Infrared Spectroscopy (FTIR).

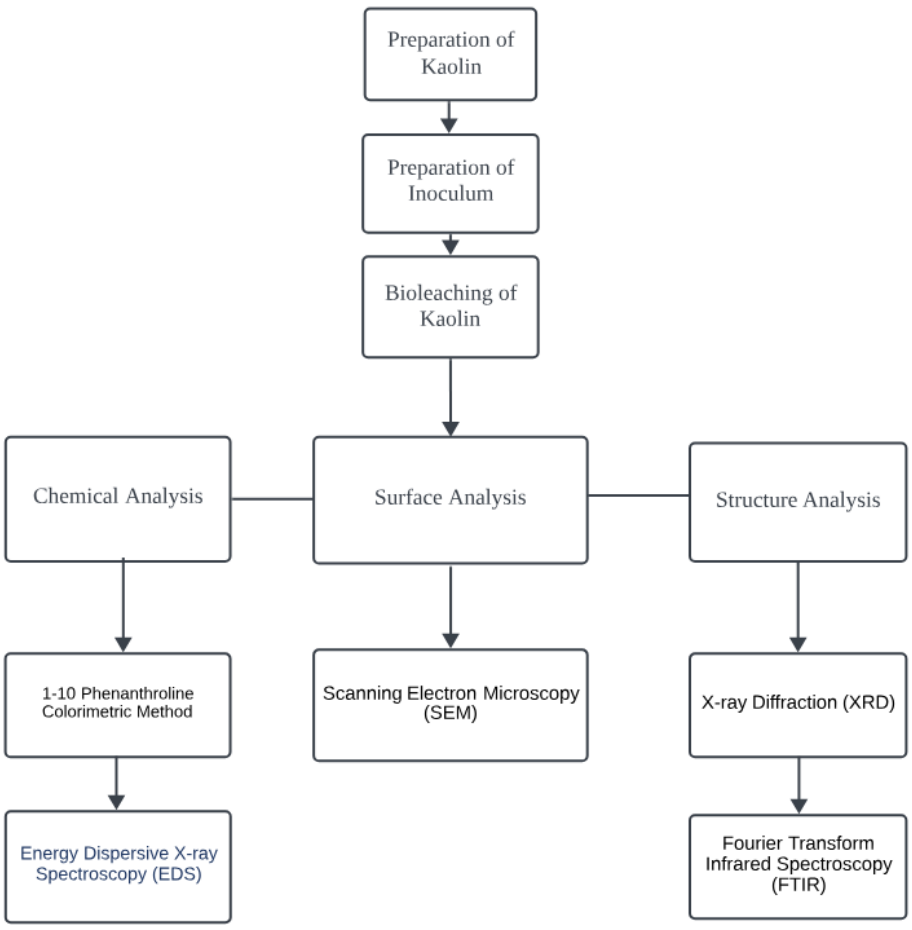

Figure 3.1: Methodology chart for bioleaching.

The experiment followed a two-stage method. Initially, bacterial cultures were prepared and introduced into conical flasks post-incubation to facilitate bioleaching of kaolin. Subsequently, the supernatant of the bioleached kaolin was subjected to phenanthroline analysis on days 0, 2, 4, 6, 8, and 10 (with 2-day intervals). Following this, the bioleaching kaolin underwent filtration using 11 µm filter paper, and the resulting residues were dried in an oven at 80°C until completely dry. These dried residues were then ground into a powder form for further analysis via SEM-EDS, XRD, and FTIR techniques. The powders from day 0, day 10, and the raw kaolin were analyzed. The experimental methodology was adapted from Lee et al. (2023), which elucidated potential iron reduction mechanisms in kaolin bioleaching by Bacillus species.

3.2 Preparation of Kaolin Sample

Table 3.1: Mineralogical structure of kaolin sample by XRF (Lee et al., 2023).

No	Element	Analysis result (%)
1.	Silica, SiO_2	49.40
2.	Aluminium, Al_2O_3	33.87
3.	Potassium, K_2O	3.54
4.	Iron, Fe_2O_3	1.21
5.	Magnesium, MgO	0.84
6.	Titanium, TiO_2	0.40
7.	Calcium, CaO	0.04
8.	Phosphorus, P_2O_5	0.03
9.	Sodium, Na_2O	0.03
10.	Hafnium, HfO_2	0.01
11.	Manganese, MnO	0.01
12.	Zirconium, ZrO_2	0.01
13.	Chromium, Cr_2O_3	< 0.01
14.	Strontium, SrO	< 0.01
15.	Sulphur, SO_3	< 0.01

The kaolin utilized in the study was sourced from a mine situated in Bidor, Perak, Malaysia. Table 3.1 outlines the mineralogical characteristics of

the kaolin sample. Its pH spanned from 4.0 to 5.5, boasting a brightness level of 76% to 80%. The average particle size ranged between 2.5 to 3.5 micrometers. To ensure uniformity, the kaolin particles were finely ground and thoroughly mixed. Preservation of the kaolin powder was managed in a dry environment. It was securely stored in a sterilized bottle in a dry location (Yong et al., 2022).

3.3 Preparation of Inoculum

According to Yong et al. (2022), the bacteria used were isolated directly from the kaolin sample. Subsequently, the microbes were recognized as *B. cereus* UKMCC1150, *B. aryabhattai* UKMCC1151, and *B. megaterium* UKMCC1152. This identification was achieved by employing the 16 s rRNA sequencing method, following the procedure outlined in Yap et al. (2020). Bacteria isolates are identified through the amplification of the 16S rRNA partial sequence using universal primers 27F and 1492R, followed by sequencing and analysis using BLASTn. In the case of the UKMTAR-4 strain, it was found to have high homology to Bacillus through 16S rRNA partial sequence analysis. The phylogenetic tree constructed with sequences from different Bacillus species clustered the UKMTAR-4 strain with other Bacillus cereus strains, indicating its similarity and classification as B. cereus strain UKMTAR-4. In this experiment, *B. cereus* was chosen to be used. The single colony of each bacteria was placed into Luria–Bertani (LB) broth and incubated overnight with continuous agitation at 250 rpm at 37°C.

3.4 Bioleaching of Kaolin

A 500 ml Erlenmeyer flask was used to stir 20 g of autoclaved kaolin powder and 200 mL of medium. The medium for batch 1 was 10 g/L of yeast extract. The medium for batch 2 was 10 g/L of yeast extract with an additional 10 g/L of glucose solution. Under the bioleaching process, glucose was used to assist the bacterial activity because it is the ideal nutrient source for *Bacillus* sp. (Štyriaková et al., 2003). According to Yap et al. (2020), 9×10^8CFU is the ideal concentration for the overnight cultivation of microbe. Each *Bacillus* sp. was mixed with the kaolin suspension. An incubator shaker was used to incubate the flask at 30°C, with continuous shaking at 250 rpm for 10 days (Yong et al.,

2022). The experiment was repeated in three replicate biological samples. An abiotic control sample was included under the same environment as the live bacteria samples for comparison. The total was 4 samples for each batch.

3.5 Chemical Analysis

3.5.1 1-10 Phenanthroline Colorimetric Method

The Fe (II) content was assessed every two days utilizing the 1,10-phenanthroline colorimetric technique to determine the concentration of iron removed from the kaolin. Following the collection of the kaolin mixture, centrifugation was performed prior to measurement. For the colorimetric reagent, 200 µL of 0.8% 1,10-phenanthroline solution and 200 µL of 1.28 M ammonium acetate were combined, while the complexing reagent consisted of 500 µL of 0.4 M sodium fluoride. After vortexing the mixture, 100 µL of the sample supernatant was inserted and vortexed again. Following a one-hour incubation in darkness, three aliquots of the solution, each measuring 200 µL, were relocated to a 96-well microtiter plate and analyzed using an ELISA microplate reader (Tecan, SunriseTM) at 492 nm.

3.5.2 Energy Dispersive X-ray Spectroscopy (EDS)

The chemical composition was studied by using energy-dispersive X-ray spectroscopy (EDS) (Yap et al., 2020). It operates together with the SEM, they use same scanning speed 30 frames per second (fps). Other settings are defaulted by the UTAR staff. It operates by bombarding the sample with high-energy electrons, which in turn emit X-rays that are characteristic of the elements present in the sample. These X-rays are then detected and analyzed to identify the elements and quantify their concentrations.

The mineral composition of the kaolin such as Al, K, Fe, O, and Si was analysed before and after the experiment. There are 3 samples of data of element weight collected for each type (eg. Raw kaolin, abiotic control sample, *B. cereus1-6)*. The raw data was collected as shown in Appendix A. Then, find the averages for each type. The bioleaching efficiency in EDS analysis was

calculated by the changes in Fe composition before and after bioleaching as shown in Equation 3.1.

$$Bioleaching\ efficiency\ (\%) = \frac{X_i - X_f}{X_i} \times 100\% \qquad (3.1)$$

Where,

X_i = weight percentage (wt %) of Fe composition in kaolin before bioleaching

X_f = weight percentage (wt %) of Fe composition in kaolin after bioleaching

3.6 Surface Analysis

To eliminate absorbed moisture, the kaolin suspension was subjected to air drying in an 80 °C oven for 24 hours before conducting any analyses. This was done to guarantee that the samples were completely dry and powdered.

3.6.1 Scanning Electron Microscopy (SEM)

The surface morphology of kaolin was examined both before and after bioleaching to observe the effects of iron removal, employing a scanning electron microscope (SEM) model Hitachi S-3400N. The SEM operated at a scanning speed of 30 fps, coupled with an energy dispersive X-ray spectroscopy (EDS) system Ametek Apollo X. To prepare the samples, one side of the stub was coated with double-sided sticky carbon tape, onto which dried kaolin powder was evenly spread. Prior to analysis, the samples were sealed with a layer of gold.

3.7 Structure Analysis

3.7.1 X-ray Diffraction (XRD)

For XRD analysis (Shimadzu, XRD6000), the dried sample was front-loaded, mounted, and filled at random into an empty sample holder. Cu K radiation (40 kV, 40 mA), with a step width of 0.05° and a notional collection period of 15 s per step, was used to capture the XRD patterns across a range of 10 to 80° 2θ. To compare the XRD patterns of the treated and untreated samples, the influence of bioleaching on the structural modification of the kaolinite before and after bioleaching was examined.

3.7.2 Fourier Transform Infrared Spectroscopy (FTIR)

The dried treated specimen was positioned on the FTIR (Fourier Transform Infrared Spectroscopy) sample holder of the Nicolet IS10 instrument to capture infrared absorption spectra using the OMNIC software. This method aimed to gain a deeper insight into the mechanism of bacterial cell adhesion to kaolin particles by analysing the bonding between the mineral surface and bacteria during the bioleaching process. FTIR spectra were acquired in transmission mode within the mid-infrared range of 400 to 4000 cm^{-1} using an attenuated total reflection (ATR) diamond crystal, with 100 scans performed on the spectrometer.

3.8 Summary

The methodology comprised two primary components: the bioleaching of kaolin using prepared reagents, microbes, and nutrients, and the subsequent investigation of kaolin before and after bioleaching. The experiment aimed to identify the optimal types of nutrients, specifically pure yeast extract and a combination of yeast extract and glucose solution, by assessing the iron removal rate and structural changes in kaolin. Each batch was conducted with three replicate biological samples for each nutrient type to ensure robustness and reliability in the results.

Table 3.2: Experimental Design

Batch .no	Microbe	Nutrient	Replicates	Codes
1	9×10^8CFU *B. cereus*	10 g/L of yeast extract	3	*B. cereus 1-3*
2	9×10^8CFU *B. cereus*	10 g/L of yeast extract and 10 g/L of glucose solution	3	*B. cereus 4-6*

Table 3.2 shows the experimental design for the bioleaching of kaolin. Batch 1 serves as a control or baseline condition. The inoculum consists of

9×10^8 CFU of *B. cereus,* a a bacterial species commonly found in soil and food. The nutrient medium contains 10 g/L of yeast extract, which provides a complex mixture of essential nutrients, including vitamins, amino acids, and growth factors, necessary for bacterial growth. Three replicates are included, labelled as *B. cereus 1-3*, to account for experimental variability and ensure reproducibility of results. This batch aims to observe the growth or behavior of *B. cereus* under standard nutrient conditions without any additional carbon source.

For batch 2, the inoculum level and microorganism remain the same as in Batch 1, with 9×10^8 CFU of *B. cereus*. However, the nutrient medium is modified to include both 10 g/L of yeast extract and 10 g/L of a glucose solution. The addition of glucose, a readily metabolizable carbon source, aims to study the potential influence of supplementary carbon availability on the growth or behavior of *B. cereus*. Like Batch 1, three replicates are included, labelled as *B. cereus 4-6*, to ensure statistical reliability. By comparing the results of Batch 2 with Batch 1, researchers can evaluate the effect of glucose supplementation on the microorganism's response.

Yeast extracted was used to represent the nitrogen sources and glucose solution was used to represent the carbon sources (Guo et al., 2010a). According to Guo et al. (2010a), the combination of nitrogen and carbon sources was not determined. The bioleaching efficiency of kaolin had been investigated under the glucose solution as a nutrient with *Bacillus. sp* by Lee et al. (2023), the bioleaching efficiency under the nitrogen sources and the mixture of nutrients were not analysed. In this experiment, the result focused on the bioleaching efficiency under the nitrogen sources and the mixture of nutrients with *B. cereus.*

CHAPTER 4

Result and Discussion

4.1 Introduction

In this chapter, the findings obtained from various analytical techniques employed to characterize kaolin, including SEM-EDS, XRD, and FTIR, are presented. Additionally, the results of 1-10 phenanthroline and pH analyses will be discussed. Notably, Bacillus cereus was the primary bacterial strain utilized in this study. The comparison will delve into variations in nutrient types, elucidating their impact on surface morphology, structural alterations, mineral composition, and crystallography.

4.2 Chemical Analysis

4.2.1 Phenanthroline Assay

Figure 4.1 shows the standard curve for the Phenanthroline Assay. This curve is used to determine the concentration of Fe (II) in the samples by correlating the measured absorbance values with known Fe (II) concentrations. The x-axis represents the Fe (II) concentration in micrograms per millilitre (µg/mL), ranging from 0 to 10 µg/mL. The y-axis represents the corresponding absorbance values measured during the assay.

From the data points plotted, a linear regression line has been fitted to the data. The equation of this linear regression line is $y = 0.0116x$, where y is the absorbance value, and x is the Fe (II) concentration. The correlation coefficient (R^2) value is given as 0.9972, indicating a strong positive linear correlation between the absorbance values and the Fe (II) concentrations. An R^2 value close to 1 suggests that the data points fit well to the linear regression model, and the absorbance values can be reliably used to determine the Fe (II) concentrations in unknown samples. The gradient or slope of the linear regression line is 0.0116. This value represents the change in absorbance per unit change in Fe (II) concentration. In other words, for every 1 µg/mL increase in Fe (II) concentration, the absorbance value increases by 0.0116 units.

This standard curve allows for the quantitative determination of Fe (II) concentrations in the bioleaching experiments by measuring the absorbance of the samples and using the linear regression equation to calculate the corresponding Fe (II) concentrations. It is important to note that the standard curve should be constructed using known Fe (II) concentrations and following the same experimental conditions as the actual sample measurements to ensure accurate and reliable results.

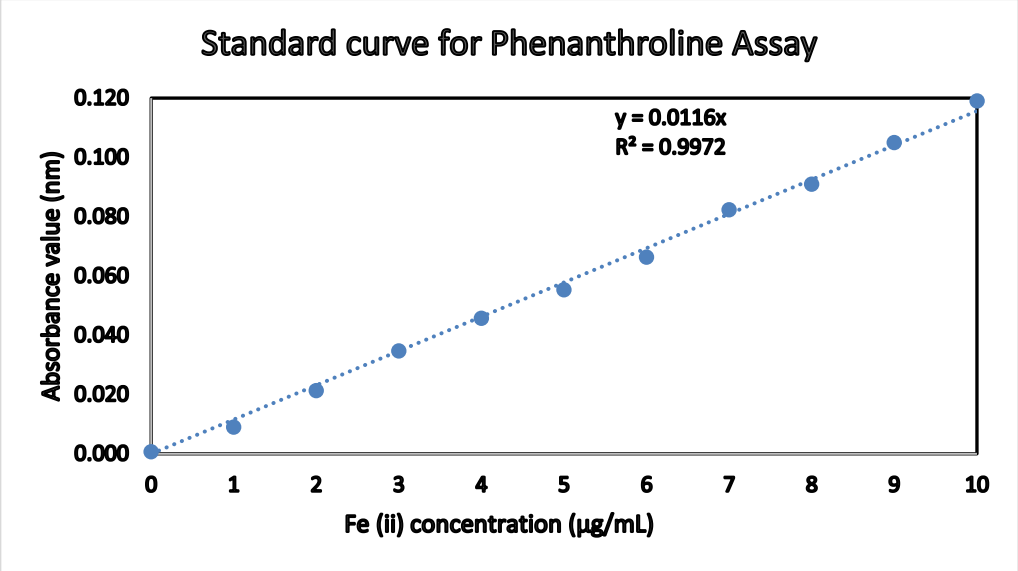

Figure 4.1: Standard curve for Phenanthroline Assay.

Figure 4.2 results showed the concentration of Fe (II) in the kaolin bioleaching system with *B. cereus* inoculation and an abiotic control over the 10-day experimental period. The Fe (II) concentration for the biotreated sample was 1.87 µg/ml on day 0. It was slightly larger than the abiotic control, which was 1.38 µg/ml. The initial Fe (II) concentration is low at the beginning of the bioleaching process.

The Fe (II) concentration for the biotreated sample gradually increases to 4.48 µg/ml on day 10. This increase in Fe (II) concentration served as an indication of the reduction of Fe (III) in the kaolin to its soluble form, Fe (II). The presence of Fe (II) indicates the reduction of iron from the kaolin material by bacterial activity. While the Fe (II) concentration of abiotic control on day 10 was slightly decreased to 0.95 µg/ml. It reached a maximum value of 2.16 µg/ml at day 6.

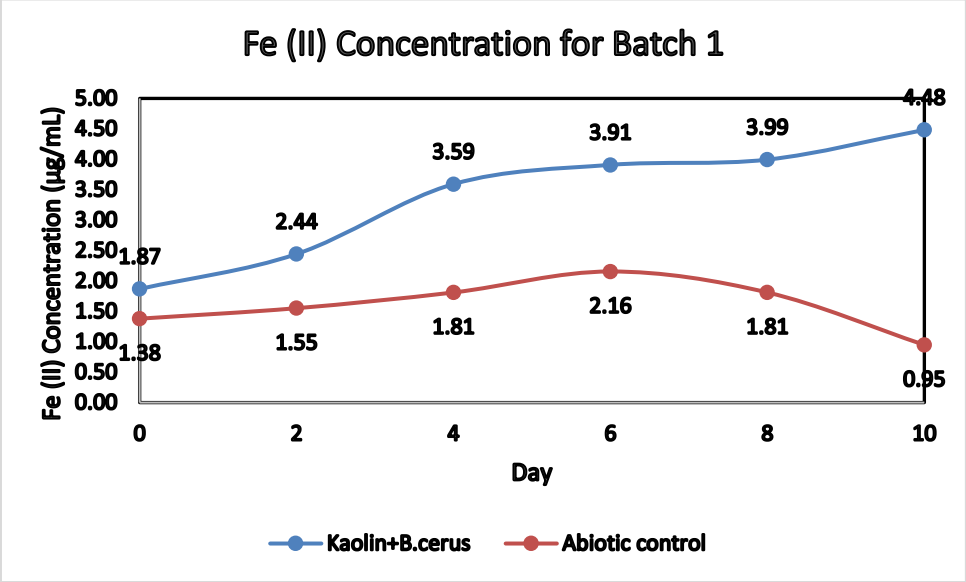

Figure 4.2: Concentration of Fe (II) in bioleaching of kaolin with *B. cereus* inoculation and an abiotic control using yeast extract as a nutrient source.

Similar to Batch 1, Figure 4.3 results demonstrated the concentration of Fe (II) in a bioleaching system with *B. cereus* inoculation and an abiotic control over the 10-day experimental period, using the yeast extract and glucose nutrient mixture.

The Fe (II) concentration for the biotreated sample was 0.92 µg/ml on day 0. It was slightly lower than the abiotic control, which was 1.06 µg/ml. The Fe (II) concentration for the biotreated sample was raised to 3.78 µg/ml on day 10. The presence of Fe (II) indicates the reduction of iron from the kaolin material by bacterial activity. While the Fe (II) concentration of abiotic control on day 10 was slightly decreased to 0.95 µg/ml. It reached a maximum value of 1.81 µg/ml at day 6.

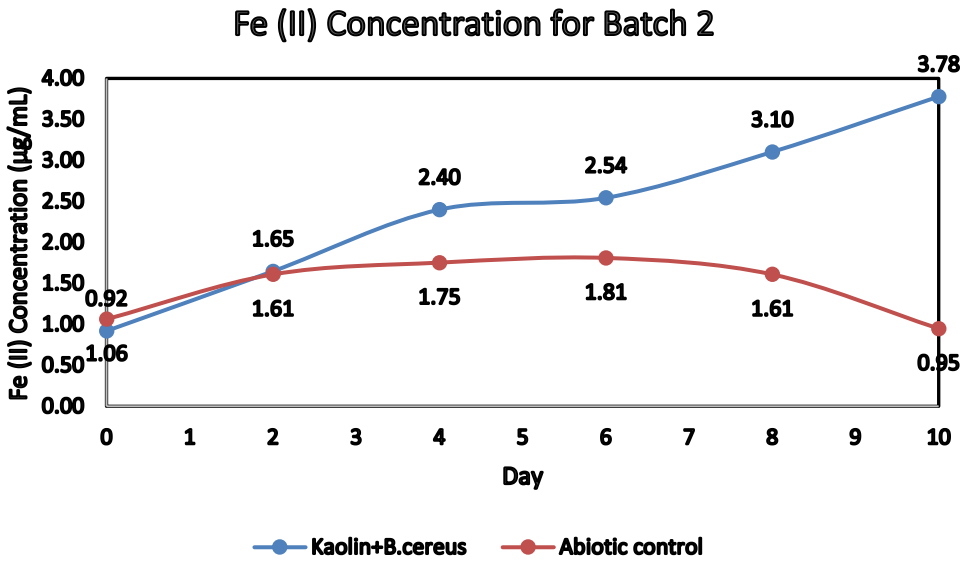

Figure 4.3: Concentration of Fe (II) in bioleaching with *B. cereus* inoculation and an abiotic control using yeast extract and glucose as nutrient sources.

In our experiments, we observed a gradual increase in Fe (II) concentration over the 10 days, indicating the reduction of Fe (III) in the kaolin matrix to its soluble form, Fe (II), facilitated by bacterial activity (Lee et al., 2023). This trend was consistent across both Batch 1 and Batch 2 experiments.

The increasing trend in Fe (II) concentration observed in the *B. cereus* cultures indicates that this bacterium is capable of reducing Fe (III) to Fe (II). This reduction could be facilitated by various mechanisms, such as the production of siderophores (iron-chelating compounds) or the presence of enzymes or metabolic pathways that facilitate iron reduction.

In Batch 1, where only yeast extract was used as a nutrient source, the Fe (II) concentration increased from an initial value of 1.87 µg/ml to 4.48 µg/ml by day 10. Similarly, in Batch 2, where glucose was supplemented in addition to yeast extract, the Fe (II) concentration increased from 0.92 µg/ml to 3.78 µg/ml over the same period. These observations indicate the efficient reduction of Fe (III) by *B. cereus*, with Batch 2 exhibiting a higher Fe (II) concentration, suggesting that the presence of glucose enhances the iron reduction processes (Lee et al., 2023).

4.2.2 pH Analysis

Figure 4.4 shows the pH analysis for yeast extract (batch 1) within 10 days. The blue line indicates the kaolin sample treated with *B. cereus* and the orange line indicates the abiotic control of the kaolin sample. The biotreated kaolin on day 0 is pH 5.01. The kaolin sample with bioleached is pH 8.57 at day 10. It reaches a maximum value of pH 8.8 at day 6. The obvious growing curve can be observed for the biotreated sample was the period from day 4 to day 6. The initial pH for abiotic control was 5.04 at day 0, while the final pH was 8.71 at day 10. It reaches a maximum value of pH 9.2 at day 6.

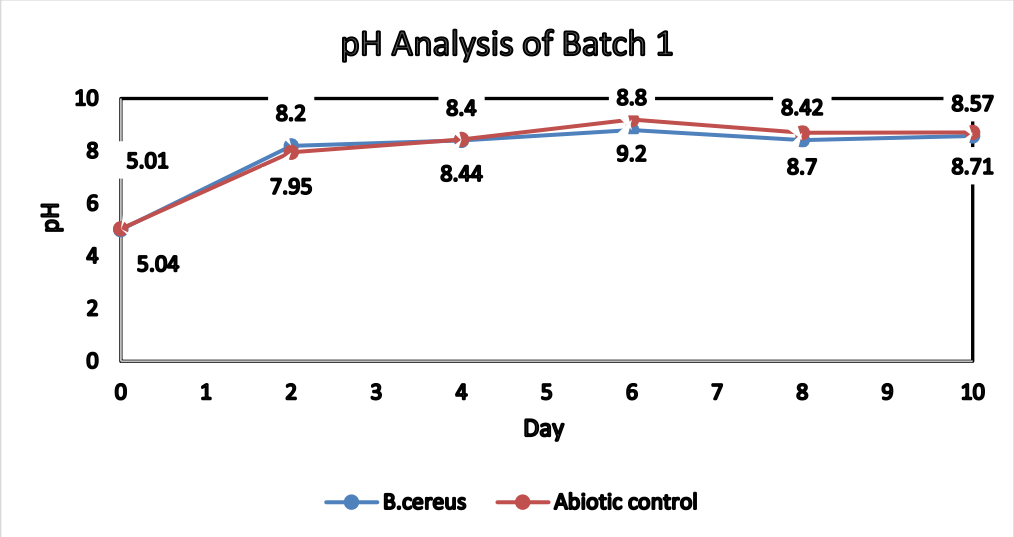

Figure 4.4: pH analysis of Batch 1.

Figure 4.5 shows the pH analysis for the mixture of nutrients (batch 2) within 10 days. The blue line indicates the kaolin sample treated with *B. cereus* and the orange line indicates the abiotic control of the kaolin sample. The biotreated kaolin on day 0 is pH 4.64. The kaolin sample with bioleached is pH 8.54 at day 10. The growth of pH for the biotreated sample showed an increasing trend as in batch 1. The obvious growing curve can be observed for the biotreated sample was the period from day 4 to day 6. The initial pH for abiotic control was 4.64 at day 0, while the final pH was 4.63 at day 10. The abiotic control remained normal, it did not show much changes from day 0 to day 10.

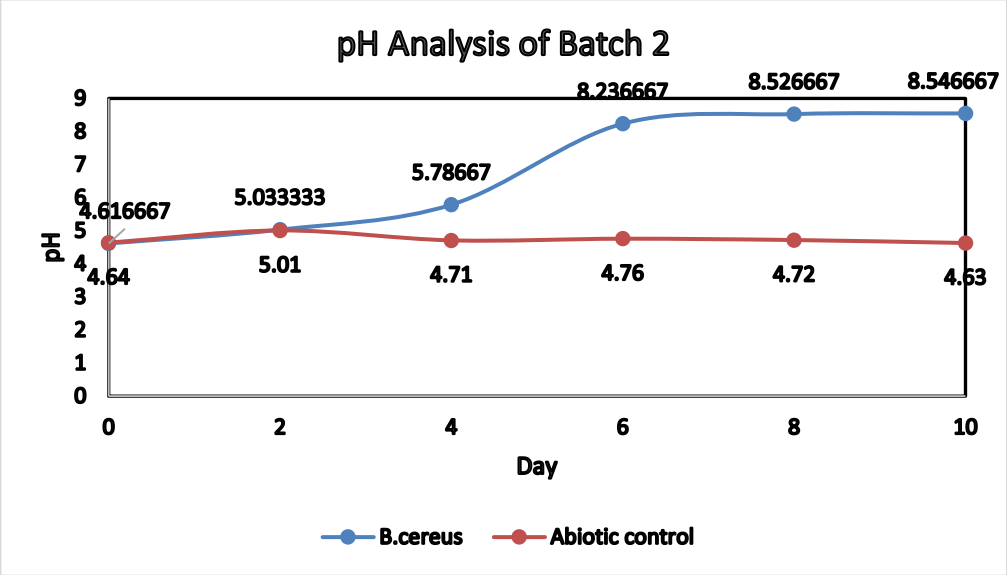

Figure 4.5: pH analysis of Batch 2.

The growing pH in yeast, particularly *Debaryomyces hansenii*, is largely attributed to the production of ammonia during the ripening of surface-ripened cheeses. This ammonia production is a significant factor contributing to pH increases within the cheese environment (Gori et al., 2007). It is consistent with our result when using the yeast extract as a nutrient.

There appears to be a clear correlation between the production of ammonia by different yeast strains and the variations in pH observed. Different yeast species and strains exhibit varying levels of ammonia production, which in turn influences the pH changes occurring during cheese ripening. Additionally, ammonia is identified as a signalling molecule in yeasts, although its specific role in *D. hansenii* remains incompletely understood. Moreover, the substrate used by yeast species affects their production levels of ammonia. Variations in ammonia production on different media may be due to differences in the content of free amino acids, indicating that substrate composition plays a role in regulating ammonia production (Gori et al., 2007).

During bioleaching experiments involving *B. cereus*, the use of yeast extract in batch 1 has been observed to lead to an increase in pH values. Yeast extract, containing nitrogen-rich compounds, can serve as a source of nutrients for bacteria and promote their growth and metabolic activity (Guo et al., 2010a). This leads to the production of ammonia (NH_3) as a metabolic byproduct. Ammonia, being a basic compound, contributes to the rise in pH levels within

the medium. The ammonia produced from yeast extract resembles the effect seen with other nitrogen sources such as $(NH_4)_2SO_4$, beef extract, and urea. The increase in pH facilitates bacterial adhesion to the ferric oxide surface, which is crucial for the subsequent reduction of ferric ions from the kaolin substrate.

The basification occurred due to the production of ammonia as a byproduct of nutrient utilization for growth and metabolism. The pH of the medium exceeded pH 8.5 on day 6 in the research of Jing et al. (2021). It is consistent with our results. Therefore, the utilization of yeast extract, rich in nitrogen compounds that yield ammonia, plays a significant role in creating an environment conducive to bacterial activity and ferric ion reduction during bioleaching experiments.

The bioleaching experiments involve *B. cereus*, with a mixture of nutrient sources, which was the combination of yeast extract and glucose solution (batch 2). The growth of pH value had a similar trend with batch 1. But, the maximum pH value is around 8.54. It was slightly reduced as compared to batch 1, which was pH 9.2. Glucose medium, despite promoting acidic conditions, leads to poor microbial viability. However, the presence of Fe (III) oxide was found to mitigate the acidity's effect on *B. cereus* and allowed for sustained growth. This was due to the effect of the additional glucose solution (Jing et al., 2021 & Lee et al., 2023). The glucose solution caused the microbes to promote the organic acids which acidified the solution and decreased the pH value. The final optimum pH value for both batches in D10 is 8.54 even though the variation of nutrients. For the result, the influence of yeast nutrients is higher than the mixture to determine the range of pH.

This basification of the solution is attributable to the release of alkaline byproducts or metabolites, such as ammonia, generated during bacterial metabolism. Interestingly, the pH of the abiotic control solution was slightly higher than the bioleaching solution, which could be attributed to the bacteria's release of intracellular protons to maintain homeostatic balance in a limited carbon environment.

4.2.3 Energy Dispersive X-ray Spectroscopy (EDS)

Table 4.1: EDS result for bioleaching experiment batch 1 in yeast solution.

Day 0					
	Element Weight %				
	O	Al	Si	K	Fe
Raw Kaolin	47.61	19.94	27.10	3.65	1.70
Control	46.26	19.72	27.60	4.71	1.71
B. cereus	42.23	21.70	29.60	4.83	1.64
Day 10					
	Element Weight %				
	O	Al	Si	K	Fe
Control	43.20	20.90	29.01	4.87	2.01
B. cereus	49.93	20.85	26.06	2.41	0.74
Fe removal rate for *B. cereus* in batch 1					54.88

From the EDS result in Table 4.1, the data from five elements which are the contents of oxygen, aluminium, silicon, potassium and iron are collected. By focusing on the concentration of iron, the initial untreated kaolin contained higher iron concentration than the treated kaolin within the 10-day observation period. The element weight percentage of iron (Fe) for the raw kaolin sample in batch 1 (yeast condition) was 1.70%, while it decreased to 0.74% for the kaolin with treatment of *B. cereus* after 10 days of bioleaching.

At Day 0 in Batch 1 with yeast as the nutrient source, the analysis of the raw kaolin sample revealed an average Fe content of 1.70 wt% from three sample collections, while the abiotic control sample showed a similar average Fe content of 1.71 wt%. Additionally, the initial kaolin sample treated with *B. cereus* displayed a slightly lower Fe content, averaging at 1.64 wt% across three biological replicates, each consisting of three sample collections. These findings indicate comparable Fe levels between the untreated and abiotic control samples, with a slight reduction observed in the treated sample, suggesting minimal initial impact of the bacterial treatment on the Fe content of the kaolin.

By Day 10, significant changes in Fe content became evident. The abiotic control sample exhibited a notable increase in Fe content, averaging at 2.01 wt%, indicating potential oxidation or other processes affecting the mineral composition throughout the experiment. In contrast, the kaolin with treatment of *B. cereus* showed a substantial decrease in Fe content, averaging 0.74 wt% across three biological replicates. This drastic reduction suggests an effective bioleaching process mediated by *B. cereus*, resulting in the removal or transformation of Fe-containing minerals within the kaolin. Overall, the comparison between Day 0 and Day 10 highlights the dynamic nature of the bacterial treatment, with significant alterations in Fe content observed throughout the experiment.

The iron removal rate for *B. cereus* in batch 1 (yeast condition) was calculated as 54.88%, based on the decrease in Fe content from 1.64 wt% (Day 0) to 0.74 wt% (Day 10) for the treated samples.

Table 4.2: EDS result for bioleaching experiment batch 2 in mixture nutrients.

Day 0					
	Element Weight %				
	O	Al	Si	K	Fe
Raw Kaolin	47.61	19.94	27.10	3.65	1.70
Control	46.04	18.71	27.81	5.72	1.72
B. cereus	44.67	19.39	28.51	5.71	1.67
Day 10					
	Element Weight %				
	O	Al	Si	K	Fe
Control	47.44	18.61	27.36	4.95	1.66
B. cereus	51.13	19.09	25.49	3.49	0.81
Improvement for *B. cereus* in batch 2					51.55

From Table 4.2, it shows the element weight of batch 2. At Day 0 in Batch 2 with yeast and glucose as the nutrient source, initial assessments of the kaolin samples revealed consistent iron content between the raw sample, abiotic control, and *B. cereus*-treated samples. The average Fe content for the raw

kaolin sample and abiotic control was 1.70 wt% and 1.72 wt%, respectively, while the treated kaolin displayed a slightly lower Fe content of 1.67 wt%.

By Day 10, while the abiotic control sample maintained a similar iron content at 1.66 wt%, the kaolin with treatment of *B. cereus* showed a notable decrease in iron content, averaging at 0.81 wt%. This significant reduction in iron content suggests effective bioleaching activity by *B. cereus* in the presence of both yeast and glucose as nutrient sources.

The iron removal rate for *B. cereus* in batch 2 (yeast and glucose mixture) was calculated as 51.55%, based on the decrease in Fe content from 1.67 wt% (Day 0) to 0.81 wt% (Day 10) for the treated samples. The iron removal rate for yeast and glucose mixture (51.55%) is slightly decreased compared to the yeast condition (54.88%). The element weight for iron was removed from 1.64 to 0.81% in batch 1 condition (yeast), while the iron removal rate for yeast and glucose mixture is 51.55%.

In agreement with the findings of Guo et al. (2010a), our EDS analysis revealed a significant decrease in iron concentrations in the kaolin samples treated with *B. cereus* compared to the untreated samples. Guo's study also demonstrated a reduction in iron content after bioleaching, highlighting the efficacy of microbial processes in removing iron impurities from kaolin minerals. Furthermore, Guo et al. (2010a) investigated the efficiency of different carbon and nitrogen sources on iron removal from kaolin by heterotrophic iron-reducers, showing that certain carbon sources, such as monosaccharides, can effectively support biomass growth and enhance the bioleaching process. Similarly, this study suggests that *B. cereus*, when cultivated in a yeast extract medium supplemented with glucose, may utilize the available carbon and nitrogen sources to facilitate iron removal from kaolin, potentially through metabolic activities or interactions with the mineral surface. This supports the notion that nutrient mixtures, such as glucose and yeast extract, can serve as effective growth substrates for microbial-mediated bioleaching processes, leading to the removal of iron impurities from mineral substrates.

The iron removal rates of 54.65% and 51.55% for batch 1 (yeast) and batch 2 (yeast + glucose), respectively, indicate that the presence of an additional carbon source (glucose) did not significantly enhance the iron

removal efficiency by *B. cereus* in this experiment. These results reinforce the importance of nitrogen sources, such as yeast extract, in facilitating iron removal by Bacillus cereus, as observed by Jing et al. (2021).

The slightly lower iron removal rate in batch 2 could be attributed to the feed of fungi. It was because the normal surface of the kaolin suspension was smooth after filtration as Figure 4.37. Conversely, the rough surface of the kaolin suspension was shown in Figure 4.36. The raw data was collected from EDS also higher than others. It made the imbalance of the average value to calculate the iron removal rate.

Besides, other various factors influence the efficiency, such as changes in bacterial metabolism, competition for resources, or alterations in the mineral-bacteria interactions due to the presence of glucose. The removal of iron from kaolin could have implications for various industrial applications, such as improving the whiteness or brightness of the mineral for use in ceramics, paper, or pigment industries, or enhancing its catalytic properties in certain processes.

Overall, the EDS analysis provides valuable insights into the iron removal capabilities of *B. cereus* during the bioleaching of kaolin, highlighting the potential for exploring and optimizing this biological process for mineral beneficiation and other applications.

4.3 Surface Analysis

4.3.1 Scanning Electron Microscopy (SEM)

Figures 4.6 - 4.21 present the SEM analysis results for two batches of kaolin samples treated with *Bacillus cereus* under different conditions. Figures 4.6 – 4.11 show that batch 1 consists of three biological replicates (*B. cereus 1-3*) grown in a yeast extract medium, while Figures 4.14 - 4.19 show that batch 2 includes three replicates (*B. cereus 4-6*) grown in a yeast extract medium supplemented with glucose.

For each batch, the SEM images show the kaolin samples before (as shown in Figures 4.6, 4.8, 4.9, 4.14, 4.16 & 4.18) and after bioleaching (as shown in Figures 4.7, 4.9, 4.10, 4.15, 4.17 & 4.19), along with an abiotic control

sample as shown in Figures 4.12 & 4.13 and Figures 4.20 & 4.21. The images are labelled with the corresponding sample names and treatment conditions.
In Batch 1 (Yeast Extract), the kaolin samples before bioleaching and the abiotic control sample display an amorphous phase and rounded shapes, representing the initial state of the mineral in Figures 4.6, 4.8, 4.9 & 4.12. However, after bioleaching with *B. cereus 1-3*, the treated kaolin samples reveal crystalline structures and sharper edges in Figures 4.7, 4.9 & 4.10. These indicate potential mineral alterations or transformations induced by the bacterial treatment. This observation suggests that the presence of *B. cereus* in the yeast extract medium facilitated changes in the crystalline structure of the kaolin, leading to the emergence of distinct features not present in the untreated samples.

Similarly, in Batch 2 (Yeast Extract + Glucose), the abiotic control sample exhibits an amorphous phase and rounded kaolin particles, resembling the initial state observed in Batch 1 in Figures 4.14, 4.16, 4.18 & 4.20. However, upon bioleaching with *B. cereus 4-6*, grown in the glucose-supplemented medium, the treated kaolin samples display more pronounced crystalline structures and sharper edges compared to the untreated control in Figures 4.15, 4.17 & 4.19. This suggests that the addition of glucose to the nutrient medium further enhanced the bacterial bioleaching process, resulting in more significant alterations to the crystalline structure of the kaolin. Overall, the distinct transformations observed in both batches highlight the role of *B. cereus* in inducing changes to the kaolin mineral structure, with variations in nutrient composition influencing the extent of these alterations.

The SEM results indicate that the initial untreated kaolin showed an amorphous phase and round shapes, while the treated kaolin samples displayed crystalline structures and sharper edges, suggesting potential alterations or transformations induced by the *B. cereus* treatment. The observed changes in the kaolin morphology and crystalline structure after bioleaching with *B. cereus* could be attributed to the metabolic activities and interactions between the bacteria and the kaolin mineral. Consistent with the findings of Lee et al. (2023), SEM images revealed visibly sharper and slightly damaged edges of kaolin particles after bioleaching with *B.cereus*. This indicates direct bacterial

influence on the kaolin surface, suggesting that bacterial activity likely played a significant role in altering the morphology and structure of the kaolin particles.

The presence of glucose in Batch 2 may have influenced the bacterial metabolism and subsequently affected the extent or nature of the mineral transformations. The supplementation of an additional carbon source could have enhanced bacterial growth, enzyme production, or metabolic pathways involved in mineral interactions. The formation of crystalline structures and sharper edges in the treated kaolin samples suggests potential dissolution, precipitation, or recrystallization processes occurring during the bioleaching treatment. These processes could be mediated by the bacterial production of organic acids, enzymes, or other metabolites capable of interacting with the kaolin mineral.

Overall, the SEM analysis provides valuable insights into the morphological and structural changes induced by the *B. cereus* treatment on kaolin minerals, opening avenues for further investigation into the mechanisms and potential applications of this bioleaching process.

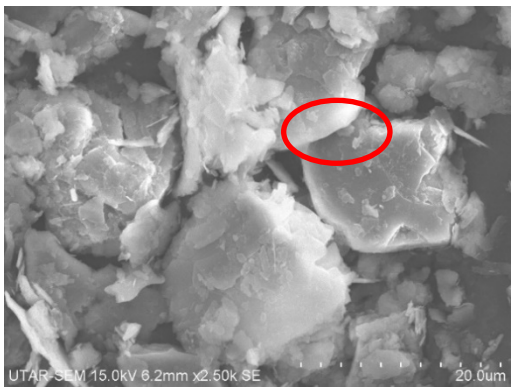

Figure 4.6: Kaolin treated with *B.cereus 1* before bioleaching in Batch 1 (D0).

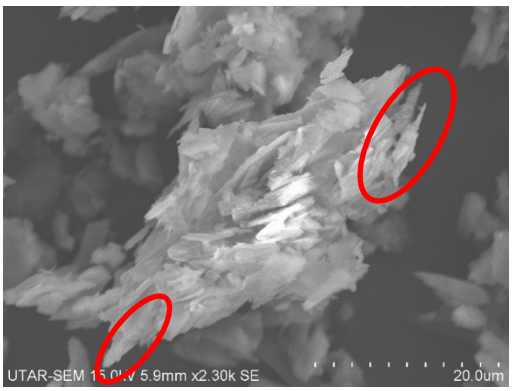

Figure 4.7: Kaolin treated with *B.cereus 1* after bioleaching in Batch 1 (D10).

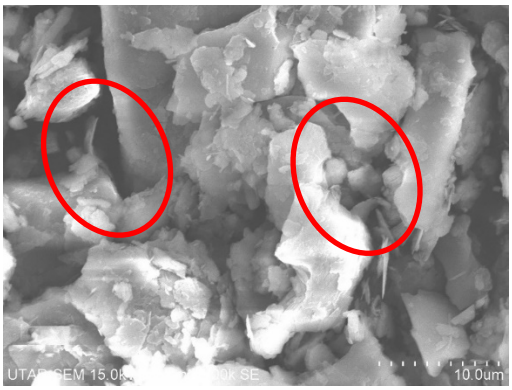

Figure 4.8: Kaolin treated with *B.cereus 2* before bioleaching in Batch 1 (D0).

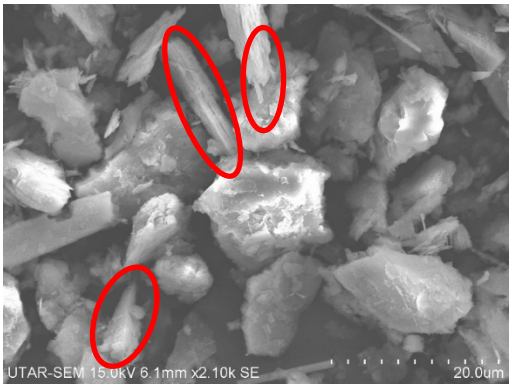

Figure 4.9: Kaolin treated with *B.cereus 2* after bioleaching in Batch 1 (D10).

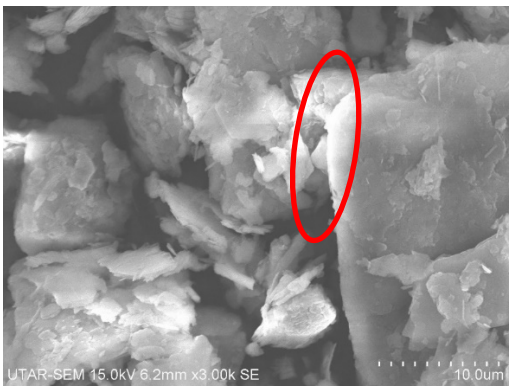

Figure 4.10: Kaolin treated with *B.cereus 3* before bioleaching in Batch 1 (D0).

Figure 4.11: Kaolin treated with *B.cereus 3* after bioleaching in Batch 1 (D10).

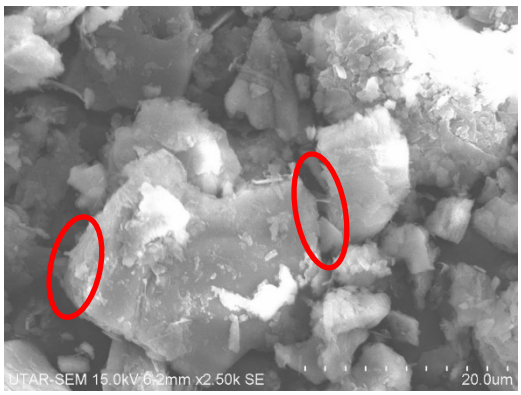

Figure 4.12: Abiotic control sample before bioleaching in Batch 1 (D0).

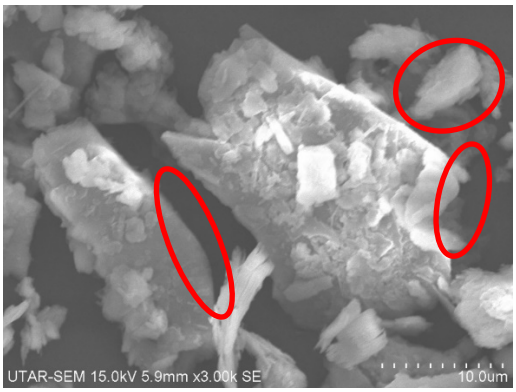

Figure 4.13: Abiotic control sample after bioleaching in Batch 1 (D10).

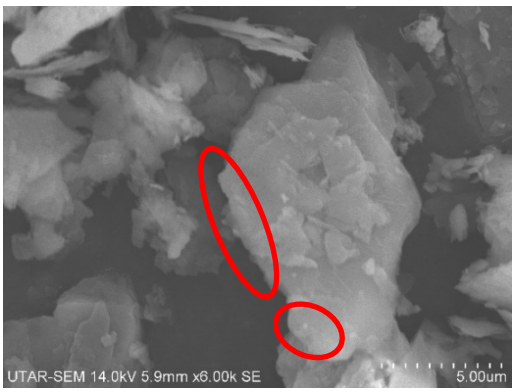

Figure 4.14: Kaolin treated with *B.cereus 4* before bioleaching in Batch 2 (D0).

Figure 4.15: Kaolin treated with *B.cereus 4* after bioleaching in Batch 2 (D10).

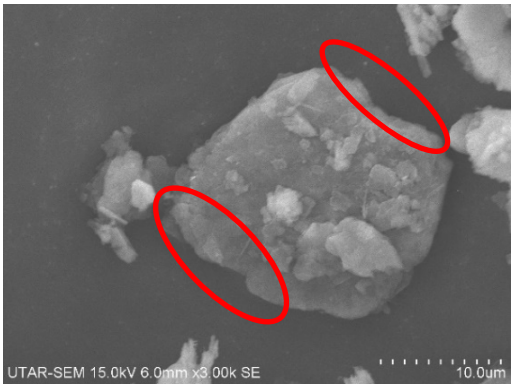

Figure 4.16: Kaolin treated with *B.cereus 5* before bioleaching in Batch 2 (D0).

Figure 4.17: Kaolin treated with *B.cereus 5* after bioleaching in Batch 2 (D10).

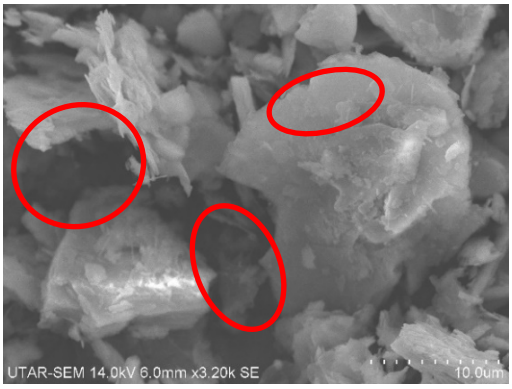

Figure 4.18: Kaolin treated with *B.cereus 6* before bioleaching in Batch 2 (D0).

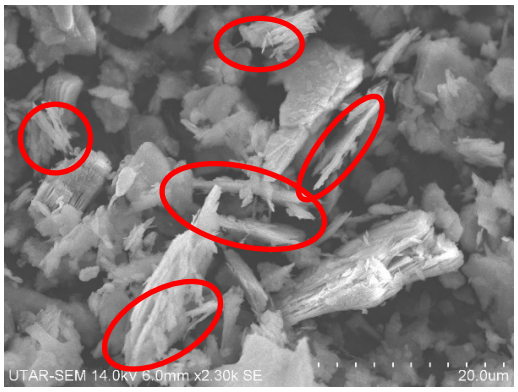

Figure 4.19: Kaolin treated with *B.cereus 6* after bioleaching in Batch 2 (D10).

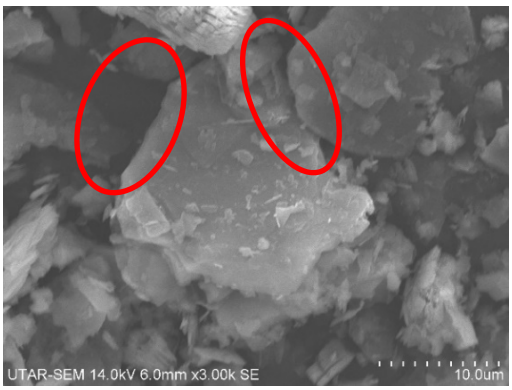

Figure 4.20: Abiotic control sample before bioleaching in Batch 2 (D0).

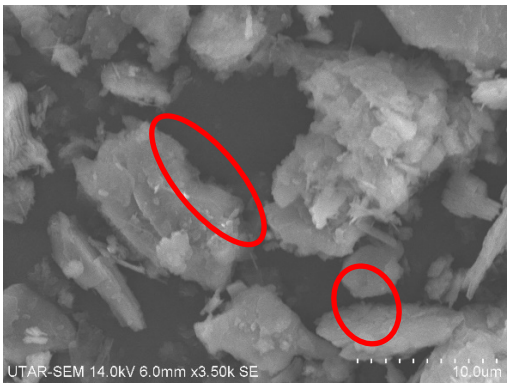

Figure 4.21: Abiotic control sample after bioleaching in Batch 2 (D10).

4.4 Structure analysis

4.4.1 X-ray Diffraction (XRD)

Figure 4.22 shows XRD patterns for untreated kaolin in Batch 1. The y-axis represents the intensity, while the x-axis represents the 2 theta angle values ranging from 10° to 80°. The blue line represents the untreated kaolin sample, which exhibits several characteristic peaks at specific 2 theta angles, indicating the presence of crystalline phases in the material.

Figure 4.23, 4.24 & 4.25 show XRD patterns for kaolin with treatment of *B. cereus 1, 2& 3* in Batch 1 after 10 days. The orange line represents the kaolin with treatment of *B. cereus 1*, the red line represents the kaolin with treatment of *B. cereus 2*, and the green line represents the kaolin with treatment

of *B. cereus 3.* They show a similar overall pattern to the untreated sample, but with some notable differences in peak intensities and positions.

The major peaks for both samples are located at approximately 12.36°, 24.9°,and 26.96° among the 2theta angles. The peak sequences from the highest to the lowest are followed by 12.36°, 24.9°,and 26.96°. These peaks are characteristic of the kaolin mineral structure and correspond to its crystallographic planes. However, the intensities of these peaks differ between the untreated and treated samples, suggesting that the treatment with *B. cereus 1* may have led to some changes in the crystalline structure or composition of the kaolin. For instance, the peak around 12.36° appears to be more intense in the treated sample compared to the untreated sample, the intensity of 12.36° for the treated sample is 2064 in Figure 4.23 and the untreated sample is 1164 in Figure 4.22. While the peak at 26.96° is less intense in the treated sample and untreated sample, which are 1232 and 600.

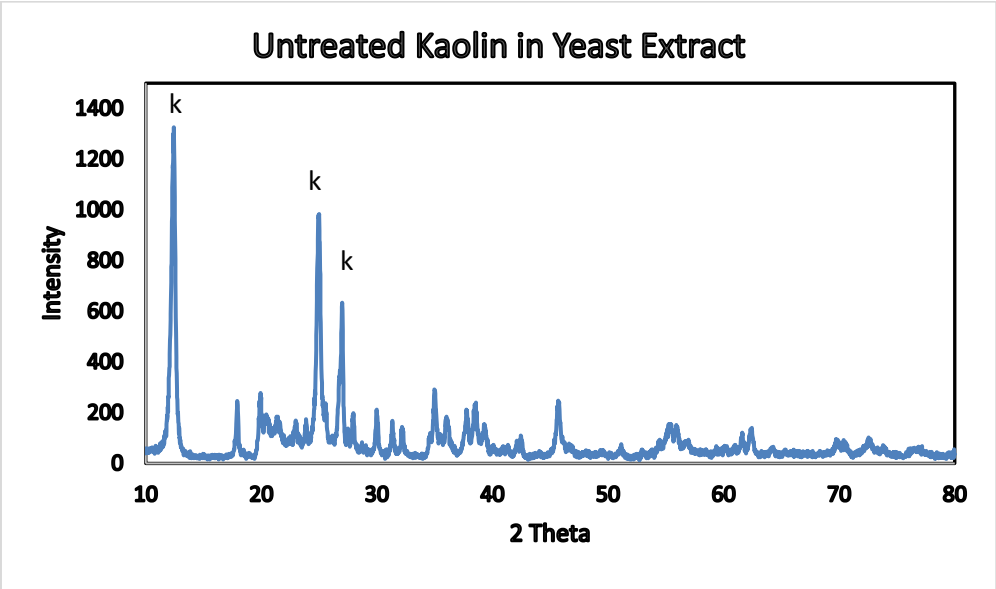

Figure 4. 22: XRD patterns for untreated kaolin in Batch 1.

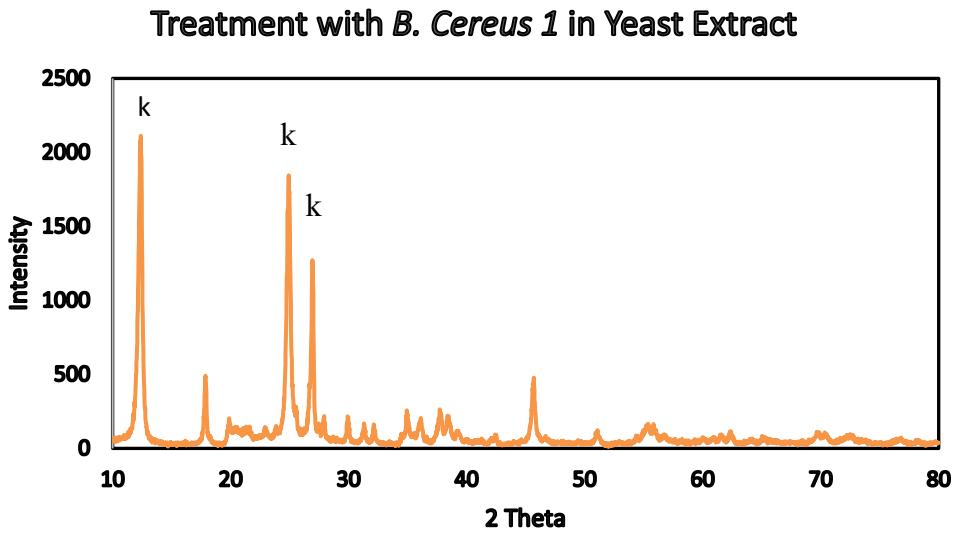

Figure 4. 23: XRD patterns for kaolin with treatment of *B. cereus 1* in Batch 1.

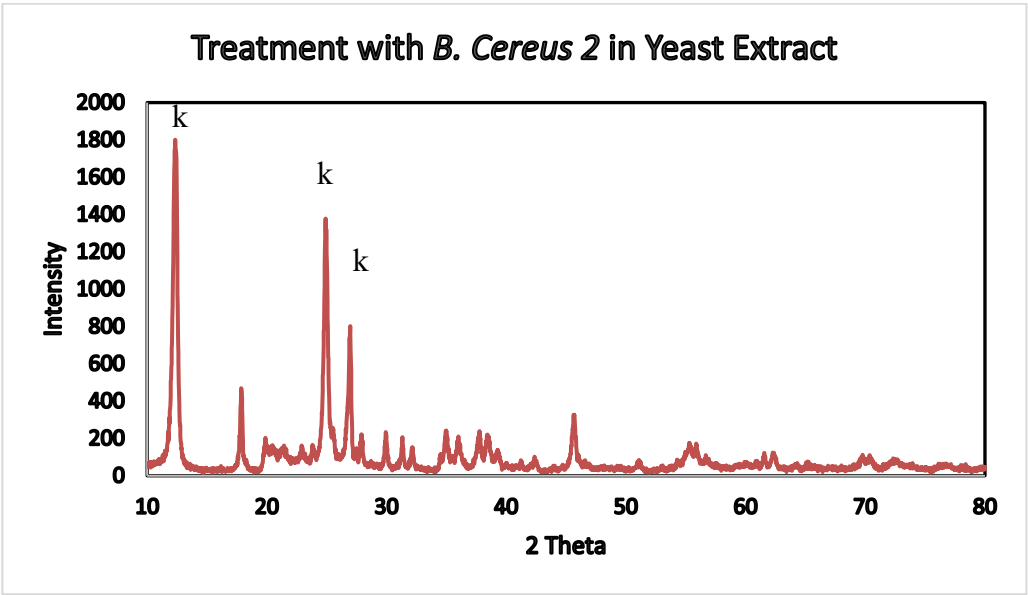

Figure 4. 24: XRD patterns for kaolin with treatment of *B. cereus 2* in Batch 1.

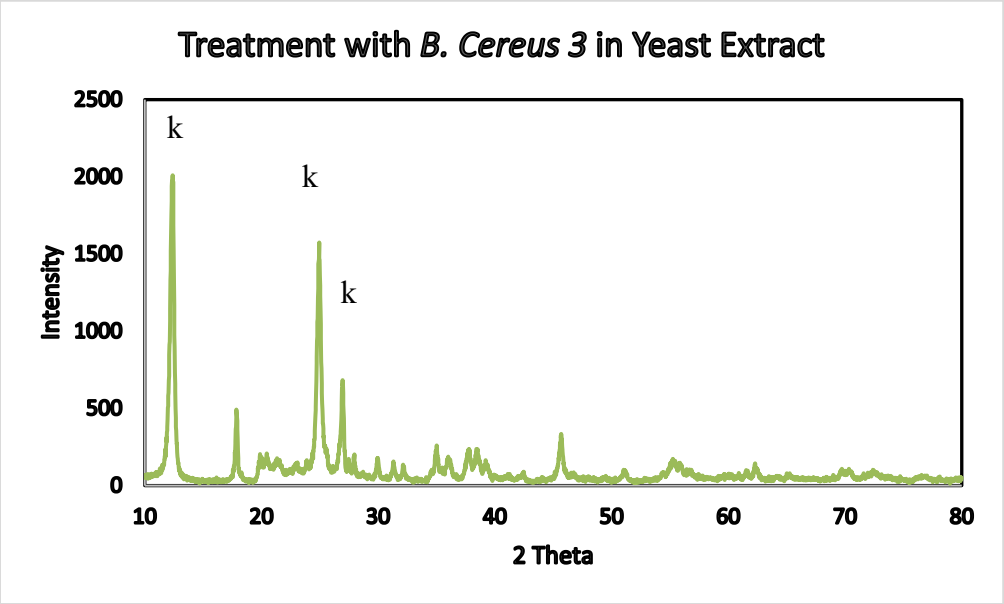

Figure 4. 25: XRD patterns for kaolin with treatment of *B. cereus 3* in Batch 1.

Figure 4.26 shows XRD patterns for untreated kaolin in Batch 2. The y-axis represents the intensity, while the x-axis represents the 2 theta angle values ranging from 10° to 80°. The blue line represents the untreated kaolin sample, which exhibits several characteristic peaks at specific 2 theta angles, indicating the presence of crystalline phases in the material. The overall pattern of batch 2 in Figure 4.26 is slightly higher than batch 1 in Figure 4.22.

Figure 4.23, 4.24 & 4.25 show XRD patterns for kaolin with treatment of *B. cereus 4, 5 & 6* in Batch 2 after 10 days. The orange line represents the kaolin with treatment of *B. cereus 4*, the red line represents the kaolin with treatment of *B. cereus 5*, and the green line represents the kaolin with treatment of *B. cereus 6.* They show a similar overall pattern to samples in batch 1, but with some notable differences in peak intensities and positions. The major peaks for both samples are located at approximately 12.42°, 24.92°,and 26.98°among the 2theta angles. The peak sequences from the highest to the lowest are followed by 12.42°, 24.92° and 26.98°.

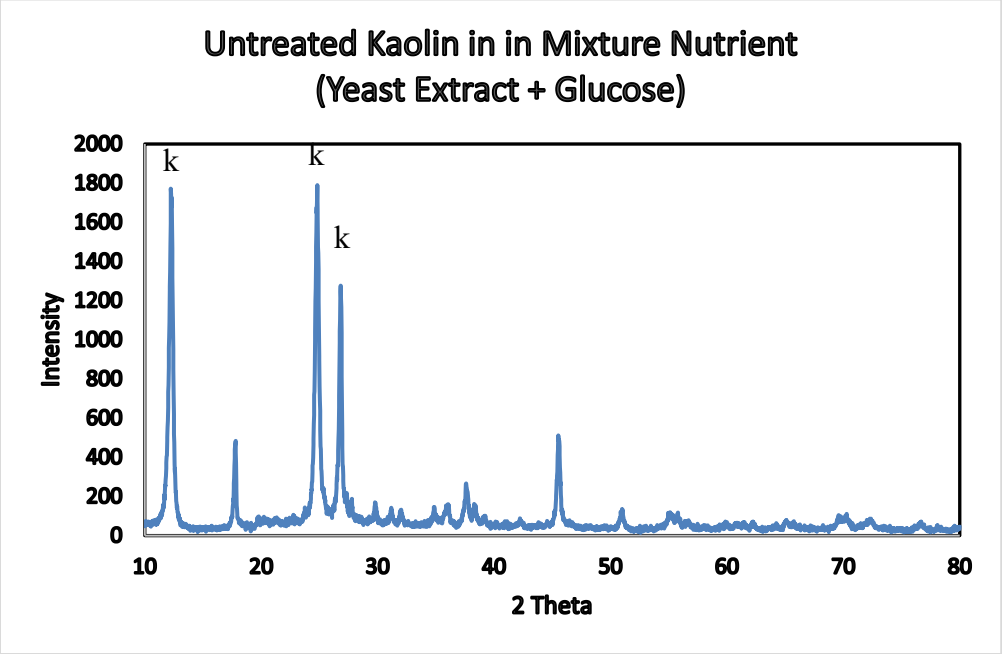

Figure 4. 26: XRD patterns for untreated kaolin in Batch 2.

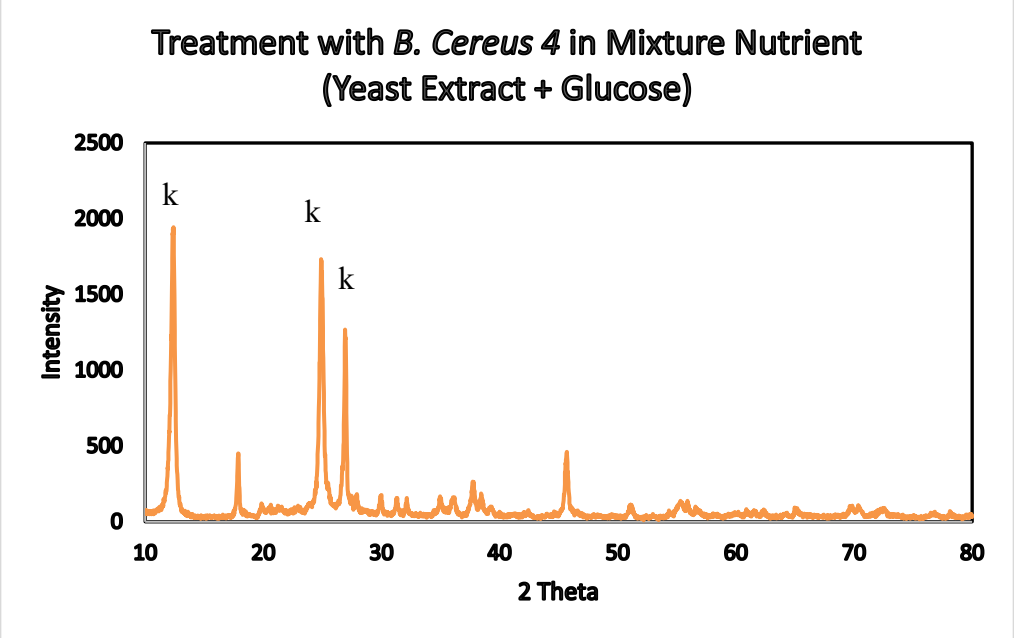

Figure 4. 27: XRD patterns for kaolin with treatment of *B. cereus 4* in Batch 2.

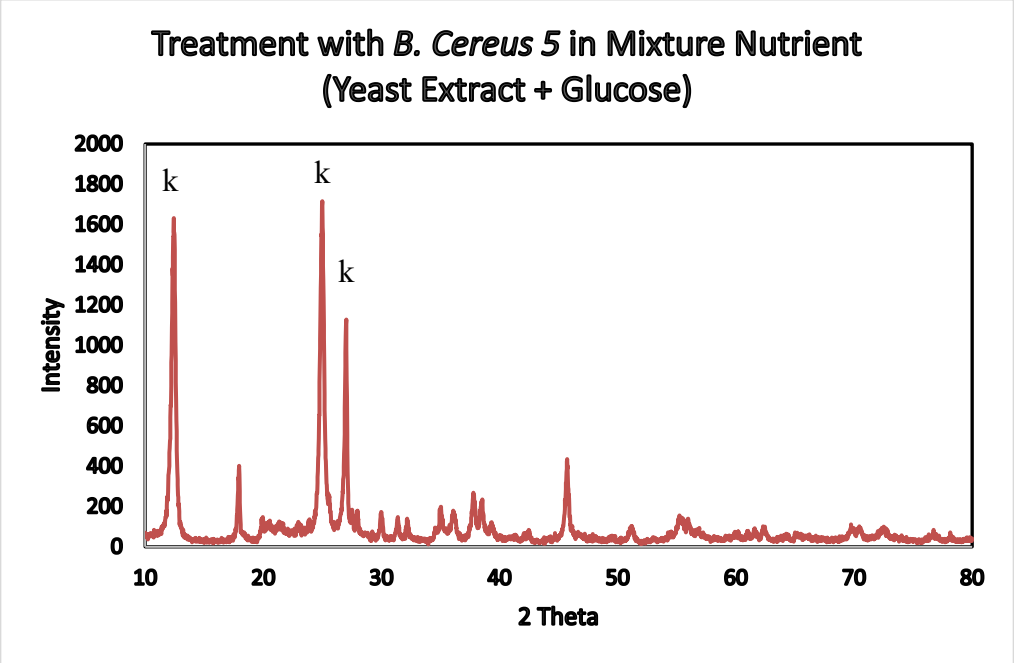

Figure 4. 28: XRD patterns for kaolin with treatment of *B. cereus 5* in Batch 2.

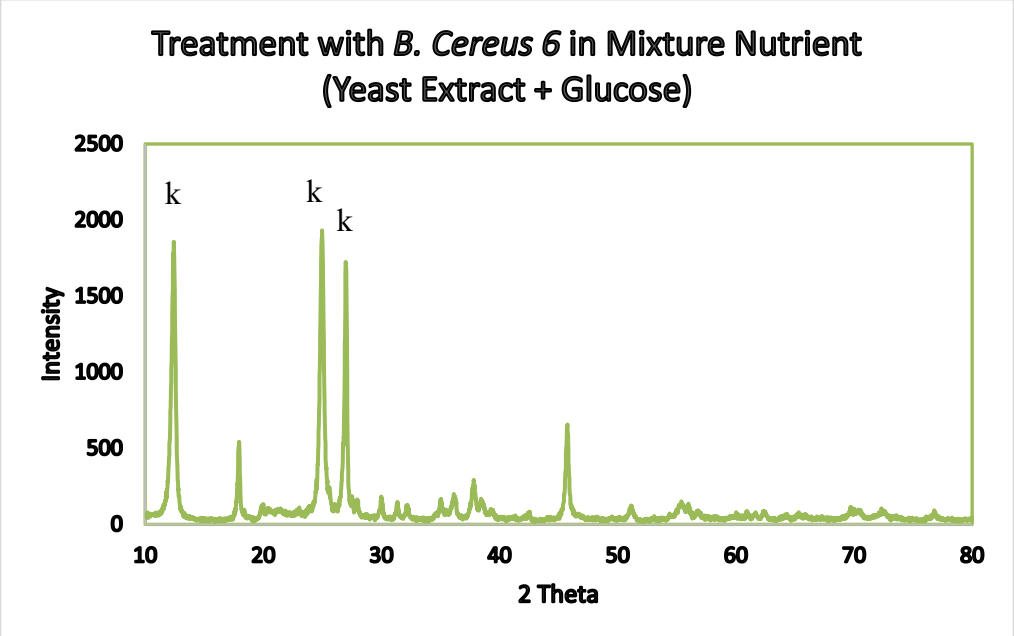

Figure 4. 29: XRD patterns for kaolin with treatment of *B. cereus 6* in Batch 2.

Based on the XRD analysis comparing untreated and treated kaolin samples with *B. cereus* in different nutrient media, several observations and implications can be discussed. Across all experiments, treated kaolin consistently displayed higher peak intensities compared to untreated kaolin, indicating potential changes in the crystalline structure or composition induced

by the bacterial treatment in Figures 4.23 - 4.25 & 4.27 – 4.29. This increase in intensity is attributed to the bioleaching process, which involves microbial-mediated extraction of elements from minerals, leading to a partial breakdown of mineral structures and consequent dissolution. As a result, the intensity of diffraction lines increases. The XRD analysis revealed negligible alterations in the crystal structure of the mineral composition between untreated kaolin and the kaolin with treatment of *B. cereus* (Lee et al., 2023). While some diffraction lines of kaolinite showed lower intensities in the treated sample, indicating potential changes in crystallinity, the overall mineral composition remained largely unaffected.

Moreover, when comparing batch 1 (yeast extract) and batch 2 (yeast extract + glucose solution) as nutrient sources, the overall intensity for batch 2 was observed to be lower after treated with *B. cereus*. This variation in nutrient sources likely influenced the efficiency of the treatment process, leading to differences in peak intensities. To address this, optimization of nutrient sources by adjusting their composition or concentration could enhance bacterial activity and improve treatment efficiency. Additionally, consideration of environmental factors such as pH, temperature, and oxygen availability may further optimize treatment conditions, resulting in more consistent and effective results.

Furthermore, while the treated samples exhibited higher peak intensities suggesting potential structural modifications, no evidence of secondary mineral phase formation was observed. This finding aligns with previous studies by Guo et al. (2010a), Zegeye et al. (2013) and Lee et al. (2023), which suggests that the treatment process primarily influences the crystalline structure rather than inducing the formation of new mineral phases. The 2-theta angle for kaolinite minerals are about 12.38° and 24.98°, while the mineral quartz is located at 27°. This finding aligns with previous studies by Dewi et al. (2018). There are no much changes on 2-theta angle between the abiotic control and biotreated sample. The difference can be observed that is due to the intensity among the biotreated samples with different nutrient and abiotic samples. XRD analysis is crucial for identifying crystalline phases and evaluating structural changes induced by treatments or processes. Despite similarities in peak positions indicating common crystalline phases, differences in intensities

provide valuable insights into the effects of treatment conditions on kaolin structure and composition.

4.4.2 Fourier Transform Infrared Spectroscopy (FTIR)

The FTIR graphs are used for analyzing molecular composition and structure. They provide insights into the chemical properties of samples by identifying characteristic absorption bands corresponding to different functional groups. In these graphs, the x-axis represents the wavenumber, which is a measure of the frequency of the infrared radiation absorbed by the sample. Each functional group within the sample absorbs infrared radiation at specific wavenumbers, allowing for their identification and analysis. The y-axis, on the other hand, denotes the transmittance percentage, representing the amount of infrared radiation that passes through the sample at a given wavenumber.

A lower transmittance percentage indicates stronger absorption of infrared radiation by the functional groups present in the sample. So, the transmittance and absorption are inversely related in FTIR (Rmladmin, 2023). Peaks or bands observed in the FTIR spectra correspond to the wavenumbers where specific functional groups absorb infrared radiation, and the intensity of these peaks or bands provides information about the relative abundance of those functional groups in the sample.

Figure 4.33 shows the FTIR for the comparison of the control sample between raw kaolin in yeast extract. There were two O-H stretch bands identified, which were 3689 cm^{-1} and 3618 cm^{-1}. Others peak are 1111 cm^{-1}, 998 cm^{-1}, 907 cm^{-1}, 747 cm^{-1}, 518 cm^{-1}, and 453 cm^{-1}. The transmittance percentage of this O-H band is lowest for the raw kaolin sample, indicating the highest intensity or abundance of hydroxyl groups on the raw kaolin surface before any treatment. The abiotic control D0 sample exhibits a higher transmittance percentage for the O-H band compared to the raw kaolin, suggesting a lower intensity or abundance of hydroxyl groups initially. The abiotic control D10 sample shows a slightly higher transmittance percentage for the O-H band compared to the control D0, indicating a further decrease in the intensity or abundance of hydroxyl groups after the incubation period without the presence of *B. cereus*.

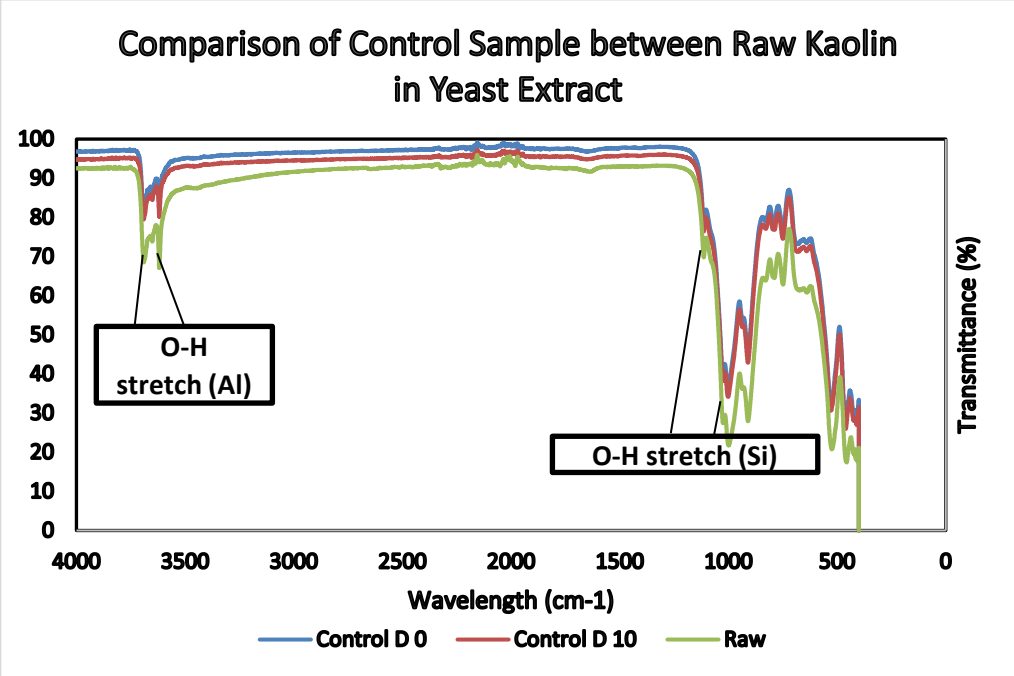

Figure 4.30: The comparison of the control samples between raw kaolin (batch 1).

Figure 4.34 – 4.36 shows FTIR for kaolin pre- and post-biotreatment of *B. cereus 1, 2& 3* in yeast extract. The O-H stretch is observed in the kaolin before and after bioleaching within 3689 cm^{-1} and 3618 cm^{-1}. However, a decrease in the transmittance percentage of the OH bands shows a reduction in the intensity of OH bands.

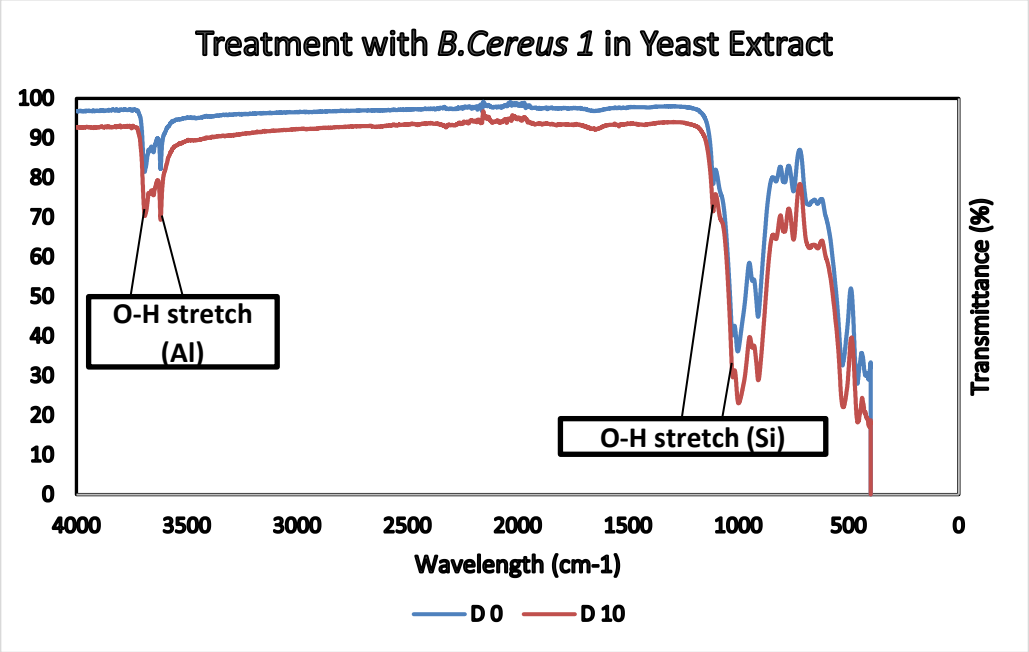

Figure 4.31: The comparison of biotreated sample 1 on D0 & D10 (batch 1).

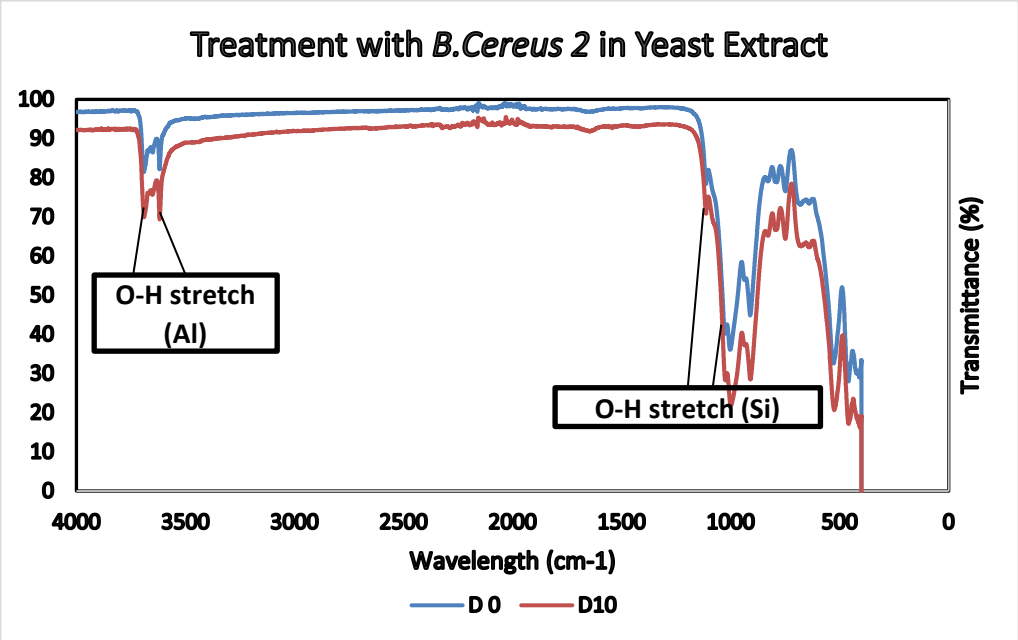

Figure 4.32: The comparison of biotreated sample 2 on D0 & D10 (batch 1).

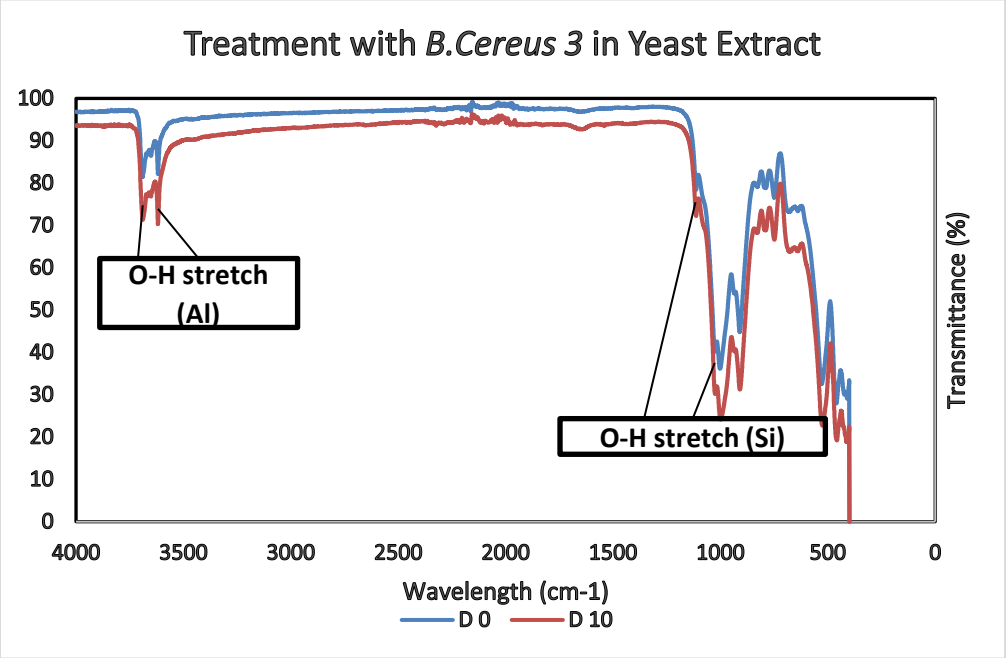

Figure 4.33: The comparison of biotreated sample 3 on D0 & D10 (batch 1).

Figure 4.37 shows the FTIR for the comparison of the control sample between raw kaolin in yeast extract and the additional glucose solution. The transmittance percentage of the raw kaolin is the lowest value as compared to the control D0 and D10. It indicates the highest initial intensity or abundance of hydroxyl groups on the raw kaolin surface. While the transmittance percentage of the control D10 has the highest value among them. The glucose solution increases the transmittance based on Figure 4.32 when the day of the experiment is increased. There were two bands identified, which were 3689 cm^{-1} and 3618 cm^{-1}. Others peak are 1111 cm^{-1}, 998 cm^{-1}, 907 cm^{-1}, 747 cm^{-1}, 518 cm^{-1}, and 453 cm^{-1}.

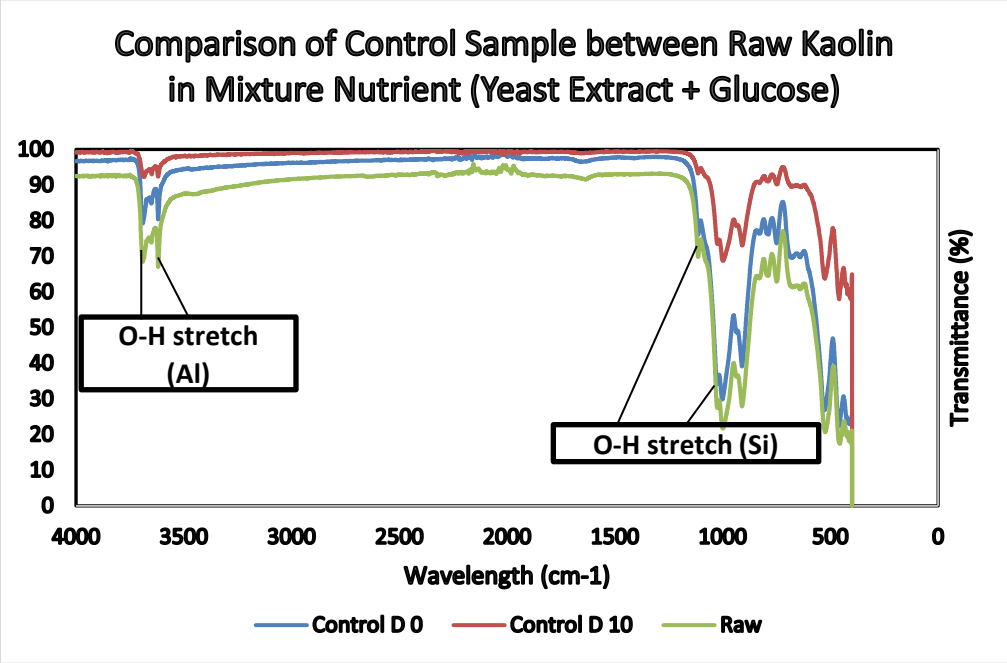

Figure 4.34: The comparison of the control samples between raw kaolin (batch 2).

Figure 4.38 – 4.40 shows FTIR for kaolin pre- and post-biotreatment of *B. cereus 4, 5& 6* in yeast extract. The O-H stretch is observed in the kaolin before and after bioleaching within 3689 cm^{-1} and 3618 cm^{-1}. However, a decrease in the transmittance percentage of the OH bands shows a reduction in the intensity of OH bands.

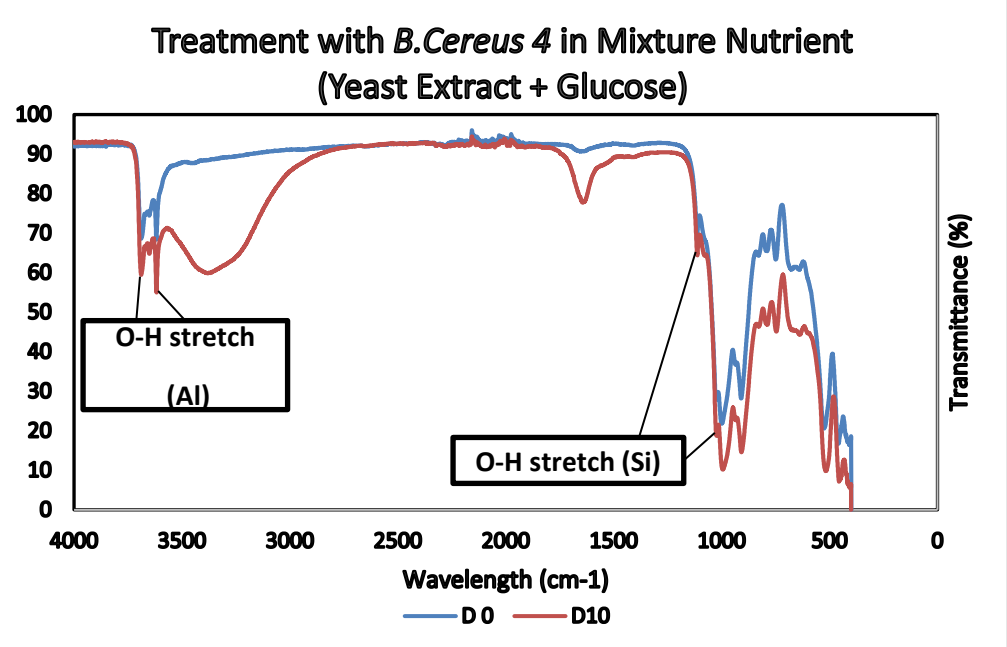

Figure 4.35: The comparison of biotreated sample 4 on D0 & D10 (batch 2).

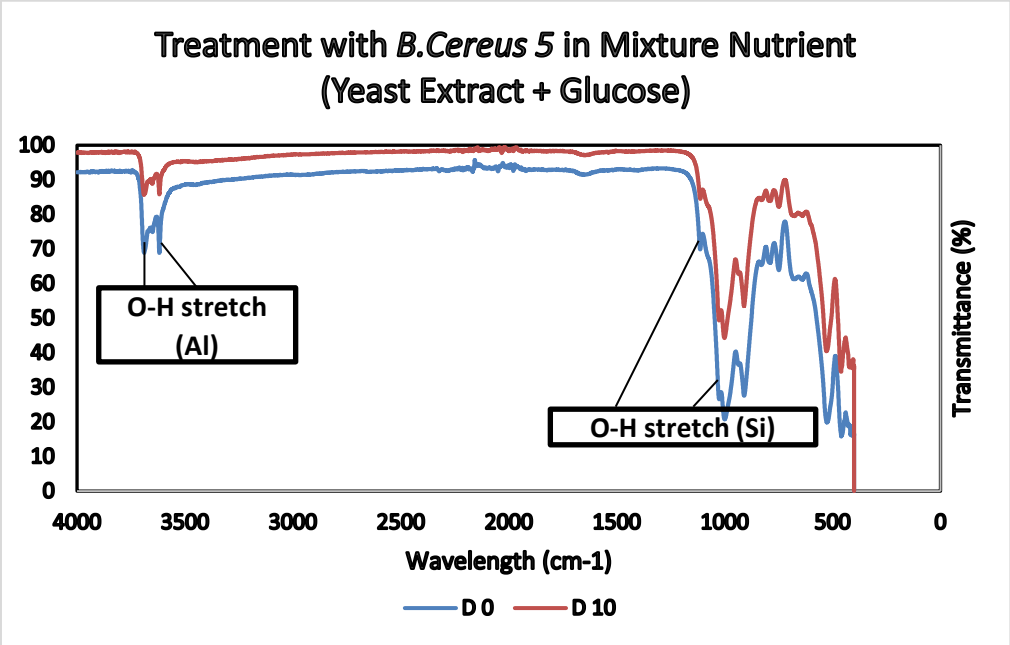

Figure 4.36: The comparison of biotreated sample 5 on D0 & D10 (batch 2).

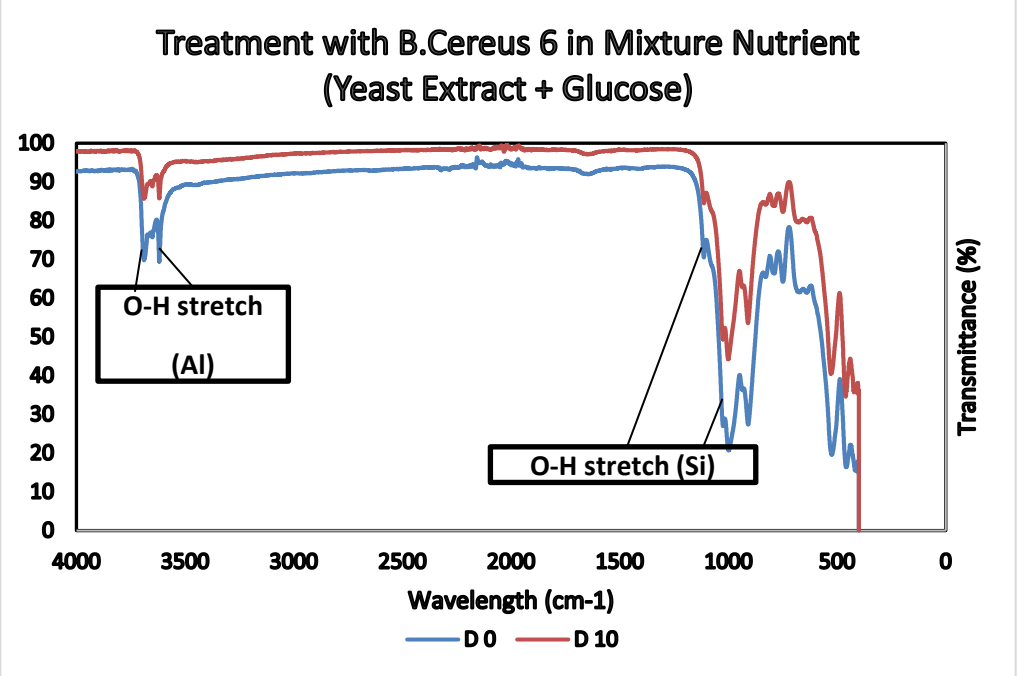

Figure 4.37: The comparison of biotreated sample 6 on D0 & D10 (batch 2).

From Figures 4.33 & 4.37, the raw kaolin sample consistently exhibits the lowest transmittance percentage for the O-H stretch band compared to the abiotic controls (D0 and D10). This common observation suggests that the raw kaolin has the highest initial intensity or abundance of hydroxyl groups on its

surface before any treatment or incubation, regardless of the medium used. Additionally, in both batches, there is a difference in the transmittance percentage of the O-H band between the abiotic controls D0 and D10, although the direction of the difference varies. This indicates that the incubation period and conditions (without the presence of *B. cereus*) can potentially influence the intensity or abundance of hydroxyl groups on the kaolin surface, albeit to a lesser extent compared to the bioleaching treatments.

Jozanikohan and Abarghooei (2022) stated that the presence of OH hydroxyls in kaolinite is located at the peak of 3696 cm^{-1}. Additional peaks at 3622 cm^{-1}, 3450 cm^{-1}, 2369 cm^{-1}, 1633 cm^{-1}, and 790 cm^{-1} are used to further confirm the presence of kaolinite in the samples. The kaolinite is detected from Iran. Variations in the source location or geological context of kaolin deposits can indeed influence the wavelength range of the characteristic absorption bands.

The O-H stretch bands within the range of 3689 cm^{-1} and 3618 cm^{-1} are consistent with the findings of Jozanikohan and Abarghooei (2022) and Lee et al. (2023). This consistency suggests that the fundamental chemical structure of kaolin remained unchanged during bioleaching with *B. cereus*. Despite bacterial interactions, the essential characteristics of kaolin, as reflected in the O-H stretch bands, remained unaffected. Therefore, the FTIR results support the stability of kaolin's chemical properties throughout the bioleaching process.

Consistent with the findings of Mohd et al. (2024), the FTIR analysis of kaolin particles revealed characteristic absorption bands in the absence of thermal activation. These included stretching vibrations of Al-O-H bonds at 3697 cm^{-1} and 3620 cm^{-1}, and deformation vibrations at 913 cm^{-1}. H-O-H stretching was observed at 3446 cm^{-1}, with bending vibrations of absorbed water at 1635 cm^{-1}. Si-O stretching exhibited out-of-plane and in-plane modes at 1115 cm^{-1}, 1031 cm^{-1}, and 1007 cm^{-1}, respectively.

Table 4.3: Summary Table for FTIR analysis.

Sample	O-H Stretch Band Range (cm^{-1})	Observation
Raw Kaolin	3689, 3618	Highest transmittance, indicating the highest initial

		abundance of hydroxyl groups before any treatment or incubation.
Abiotic Control (D0)	3689, 3618	Transmittance percentage differs from D10, suggesting that incubation conditions can influence the abundance of hydroxyl groups.
Abiotic Control (D10)	3689, 3618	Transmittance percentage differs from D0, suggesting that incubation conditions can influence the abundance of hydroxyl groups.
Batch 1 (Yeast Extract Medium), *B. cereus 1-3*	3689, 3618	Consistent decrease in transmittance percentage after bioleaching, indicating an increase in the abundance of hydroxyl groups on the kaolin surface.
Batch 2 (Mixture Nutrient Medium), *B. cereus 5 & 6*	3689, 3618	Increase in transmittance percentage after bioleaching, indicating a reduction in the abundance of hydroxyl groups on the kaolin surface.
Batch 2 (Mixture Nutrient Medium), *B. cereus 4*	3689, 3618	No significant change in transmittance percentage, potentially due to bacterial infection or experimental inconsistency.

In the FTIR spectra of kaolin with treatment of *B. cereus* in yeast extract medium (batch 1), a consistent trend emerges across the three biological replicates. The O-H stretch band is observed before and after bioleaching within the 3689 cm^{-1} and 3618 cm^{-1} range for all three replicates as shown in Table 4.3. Specifically, there is a discernible decrease in the transmittance percentage of the O-H stretch band after bioleaching. At the peak of the uptake area, the presence of vibration at 3689 cm^{-1} and 3618 cm^{-1} suggests the existence of -OH groups. These -OH groups could be bound either to aluminium octahedral atoms on the surface or within the inter-layer silicate (Dewi et al.,2018). This decrease suggests an increment in the intensity or abundance of hydroxyl groups on the kaolin surface. This distinction in environmental conditions for -OH groups indicates different chemical interactions and locations within the mineral structure. Such a phenomenon could be indicative of the removal or modification of existing hydroxyl groups during the bioleaching process. This reproducible effect underscores the potential efficacy of *B. cereus* treatment in yeast extract medium for altering the molecular composition of kaolin.

In contrast to the relatively consistent results observed in the yeast extract medium, the outcomes in the mixture nutrient medium (batch 2) exhibit variability among the biological replicates. Notably, two replicates (*B. cereus 5 & 6)* show an increase in the transmittance percentage of the O-H stretch band post-bioleaching, indicating a reduction in the intensity or abundance of hydroxyl groups on the kaolin surface. This variability in outcomes may be attributed to the additional presence of glucose in the mixture nutrient medium, which could potentially influence the bioleaching activity or mechanisms of *B. cereus* in disparate ways across the replicates.

One of the replicates (*B. cereus 4*) displays no significant change in transmittance percentage in Figure 4.38. It shows an abnormal curve, and it may be caused by the bacterial infection for D10. The possible factor for the breed of fungi is caused by closing no tie during the filtration process. This is because the protuberance of the suspension can be observed at D10 on the filter paper in Figure 4.41. If under normal conditions, the surface of the suspension is smooth in Figure 4.42. The abnormal curve in the FTIR analysis for *B. cereus 4* shows that the raw data collected from XRD lacks consistency with the others. This

inconsistency will likely lower the bioleaching efficiency, as the iron content after bioleaching is slightly higher compared to the others.

Figure 4.38: Rough surface of the suspension in D10 for biotreated sample 4.

Figure 4.39: Smooth surface of the suspension in D10 for biotreated samples in normal condition.

Upon comparing the results from Batch 1 and Batch 2, distinct trends emerge in the response of kaolin to *B. cereus* treatment in different media conditions. While *B. cereus* treatment in yeast extract medium consistently leads to a reduction in the transmittance percentage of O-H bands, indicative of an increase in hydroxyl group abundance on the kaolin surface. This variability underscores the potential influence of additional factors, such as glucose, on the bioleaching activity of *B. cereus*. However, in a mixture nutrient medium, variability in outcomes was observed among replicates, with some showing increased transmittance, possibly influenced by glucose presence affecting bioleaching activity.

The reproducible effect observed in yeast extract medium suggests that the presence of specific nutrients may play a crucial role in enhancing the bioleaching activity of *B. cereus*. Conversely, the variable outcomes in the mixture nutrient medium underscore the complexity of microbial interactions in the presence of different nutritional environments. Further investigations are warranted to elucidate the specific mechanisms underlying these observations and to explore the potential applications of *B. cereus*-mediated bioleaching in diverse industrial settings.

4.5 Summary

In summary, the bioleaching of Malaysian kaolin using *Bacillus cereus* resulted in observable morphological changes while preserving chemical bonds, as indicated by SEM and FTIR analyses. They are consistent with the studies from Lee et al. (2023) Across various analytical techniques, a substantial reduction in Fe weight percentage was noted post-bioleaching, supported by phenanthroline analysis and EDS findings. The overall results for iron removal rate under the biotreated samples with *B, cereus* are higher than the previous studies from Lee et al. (2023) with the involvement of nitrogen sources as nutrients. The iron removal rate from the studies of Lee et al. (2023) is 47.7%, while the optimum effieciency in this experiment is 54.88% with the bioleaching of *B.cereus.* Instead of optimization, this study in fact is improving the kaolin bioleaching with *B, cereus.* Despite XRD analysis confirming the unchanged mineralogy of

kaolin, the influence of nutrient type is investigated. These results are consistent with previous studies from Guo et al. (2010a) and Lee et al. (2023). The absence of ICP-OES analysis this semester due to equipment maintenance underscores the reliance on alternative methodologies. If the investigation is optimized, a better efficiency result can be expected in the further experiment.

CHAPTER 5

Conclusions and Recommendations

5.1 Conclusions

This study analysed the morphological, chemical and structural changes of kaolin bioleaching using *Bacillus. cereus.* From the analysis of the experimental results, the objective of the experiment was achieved as it was found in phenanthroline analysis that the optimum nutrient types for bioleaching kaolin with *B. cereus* are a mixture of the nutrients, the yeast extract with the combination of glucose solution. From the result shown in Figure 4.3, the highest Fe (II) concentration was increased from 1.06 µg/ml on day 0 to 3.78 µg/ml on day 10. The analysis reveals that the mixture of nutrients, specifically yeast extract combined with glucose solution, yields a higher iron concentration compared to pure yeast extract alone in the phenanthroline analysis. Consequently, this higher iron concentration contributes to increased bioleaching efficiency, as concluded from the experimental findings.

The involvement of yeast extract as a nutrient source causes the basification of the solution, so the overall pH values remain at 8.5 at D10. This is because the yeast extract is a nitrogen source. While the addition of glucose solution will slightly restrict the growth of pH value, it will acidify and neutralize the overall solution.

The result of the EDS analysis revealed that the bioleaching efficiency was slightly higher than in previous studies as Malaysian kaolin with treatment of *B. cereus* was found to be 54.88% in batch 1 and 51.55% in batch 2. The nutrient types for bioleaching experiments could be the contributing factor to the small increase in bioleaching efficiency.

For the surface analysis, it was obvious that the kaolin experienced changes in terms of structure and surface morphology after bioleaching with *B. cereus*. The SEM analysis revealed that the surface structure of kaolin increased in crystallinity. The chemical composition and bonds of kaolin remain unchanged after bioleaching as determined in the similar 12.38°, 25°, and 27° peaks of XRD analysis as well as the 3618 cm^{-1} and 3689 cm^{-1} bands of FTIR

analysis. Therefore, the last objective was also achieved in this project. In XRD analysis, 12.38° and 25° represent kaolinite minerals, while 27° represents the mineral quartz. In FTIR analysis, 3618 cm^{-1} and 3689 cm^{-1} bands represent the presence of Al.

Further optimisation of the process on a laboratory scale will be useful to render scaling-up a reality. Further investigation of optimization of nutrient types will be defined using *Bacillus* species (*B. cereus*, *B. megaterium* and *B. aryabhattai*) to find the best bioleaching efficiency among these factors.

5.2 Recommendations

Several improvements can be recommended for future studies of bioleaching. In the context of chemical composition determination within the bioleaching process of kaolin, the utilization of EDS emerges as a pragmatic substitute for ICP-OES. While ICP-OES typically offers heightened precision in elemental analysis, the deployment of EDS can effectively provide an estimation of chemical composition, albeit with a slightly lower degree of accuracy. ICP-OES downtime disrupts elemental analysis continuity, delaying data acquisition crucial for bioleaching process optimization. Given the temporary unavailability of ICP-OES due to maintenance downtime, EDS serves as a viable interim solution to ascertain elemental proportions within the bioleaching process.

The absence of precise quantification from ICP-OES poses a notable challenge in comprehensively understanding the efficiency of leaching and the dynamics of element dissolution from the kaolin matrix. Accurate elemental analysis is pivotal in gauging the efficacy of bioleaching and in fine-tuning operational parameters such as pH, temperature, microbial activity, and nutrient supplementation. Real-time insights gleaned from elemental analysis facilitate informed adjustments to these parameters, thereby optimizing kaolin dissolution efficiency while mitigating adverse environmental impacts.

To bolster the reliability and consistency of results obtained via EDS, it is imperative to implement certain procedural refinements. Firstly, ensuring thorough homogenization of the kaolin sample prior to EDS analysis is paramount to minimize variability and enhance accuracy. Additionally,

acquiring multiple replicate raw data sets from a single sample during EDS analysis and subsequently averaging these readings can mitigate potential sources of error and yield more precise estimations of chemical composition. By adhering to these methodological enhancements, the utility of EDS in facilitating elemental analysis during periods of ICP-OES downtime can be maximized, thereby sustaining the momentum of research endeavours aimed at optimizing bioleaching processes.

Furthermore, another issue such as the lack of equipment such as filtration tools will decrease the working efficiency. There are only two filtration tools and they can be used after sterilization each time. However, 4 samples are required to be filtered before further analysis. So, we only can use the alcohol to clean it after using it for the remaining samples and work under a laminar flow hood to prevent the contaminants during the experiment. By addressing these challenges, we can bolster the reliability and efficiency of bioleaching studies, ensuring robust data acquisition and advancing our understanding of this environmentally significant process.

Further investigation is recommended to optimize nutrient types for bioleaching efficiency among *Bacillus spp.*, including *B. megaterium, B. aryabhattai*, and a combination of *B. cereus, B. megaterium,* and *B. aryabhattai*. This entails systematically evaluating pure yeast extract and yeast extract combined with glucose solution across these strains to identify the most effective nutrient combination. Additionally, utilizing laboratory techniques such as SEM-EDS, FTIR, ICP-OES, XRD, and phenanthroline assay can provide insights into the structure, chemical composition, and surface analysis of the bioleaching process. Exploring the potential synergistic effects of co-culturing different *Bacillus spp.* offers the potential for enhancing efficiency, particularly through assessing mixed cultures under varying nutrient conditions. Overall, this comprehensive investigation aims to maximize bioleaching efficiency and advance the sustainable utilization of kaolin resources.

5REFERENCES

Admin, 2021. *What are the advantages and disadvantages of bioleaching? – Wise-Advices*. [online] yourwiseadvices.com. Available at: https://yourwiseadvices.com/what-are-the-advantages-and-disadvantages-of-bioleaching/ [Accessed 5 Sep. 2023].

Arslan, V. and Bayat, O., 2009. REMOVAL OF Fe FROM KAOLIN BY CHEMICAL LEACHING AND BIOLEACHING. *Clays and Clay Minerals*, 57(6), pp.787–794. doi:https://doi.org/10.1346/CCMN.2009.05706011.

Bhutia, T.K., Lotha, G., Rodriguez, E., Sinha, S., Tikkanen, A. and Young, G., 2019. Kaolin | Clay | Britannica. In: *Encyclopædia Britannica*. [online] Available at: https://www.britannica.com/science/kaolin [Accessed 15 Jul. 2023].

Bohlmann, J.T., Cameselle, C., Nunez, M.J. and Lema, J.M., 1998. Oxalic acid production by Aspergillus niger. *Bioprocess Engineering*, 19(5), pp.337–342. doi:https://doi.org/10.1007/pl00009022.

BROMFIELD, S.M., 1954. THE REDUCTION OF IRON OXIDE BY BACTERIA. *Journal of Soil Science*, 5(1), pp.129–139. doi:https://doi.org/10.1111/j.1365-2389.1954.tb02181.x.

Bundy, W.M. and Ishley, J.N., 1991. Kaolin in paper filling and coating. *Applied Clay Science*, [online] 5(5), pp.397–420. doi:https://doi.org/10.1016/0169-1317(91)90015-2.

Buyondo, K.A., Kasedde, H. and Kirabira, J.B., 2022. A comprehensive review on kaolin as pigment for paint and coating: Recent trends of chemical-based paints, their environmental impacts and regulation. *Case Studies in Chemical and Environmental Engineering*, [online] 6, p.100244. doi:https://doi.org/10.1016/j.cscee.2022.100244.

Cameselle, C., María José Núñez, Lema, J.M. and Pais, J., 1995. Leaching of iron from kaolins by a spent fermentation liquor: Influence of temperature, pH, agitation and citric acid concentration. *Journal of industrial microbiology*, 14(3-4), pp.288–292. doi:https://doi.org/10.1007/bf01569941.

Cameselle, C., Ricart, M.T., Núñez, M.J. and Lema, J.M., 2003. Iron removal from kaolin. Comparison between ‘in situ’ and ‘two-stage’ bioleaching processes. *Hydrometallurgy*, 68(1-3), pp.97–105. doi:https://doi.org/10.1016/s0304-386x(02)00196-2.

Conley, R.F. and Lloyd, M.K., 1970. Improvement of Iron Leaching in Clays. Optimizing Processing Parameters in Sodium Dithionite Reduction. *Industrial & Engineering Chemistry Process Design and Development*, [online] 9(4), pp.595–601. doi:https://doi.org/10.1021/i260036a017.

Department of Jobs, P. and R., 2021. *Kaolin*. [online] Earth Resources. Available at: https://earthresources.vic.gov.au/geology-exploration/minerals/industrial-minerals/kaolin [Accessed 15 Jul. 2023].

Dewi, R., Agusnar, H., Alfian, Z. and Tamrin., 2018. Characterization of technical kaolin using XRF, SEM, XRD, FTIR and its potentials as industrial raw materials. *Journal of Physics: Conference Series*, [online] 1116, p.042010. doi:https://doi.org/10.1088/1742-6596/1116/4/042010.

Fonti, V., Dell'Anno, A. and Beolchini, F., 2016. Does bioleaching represent a biotechnological strategy for remediation of contaminated sediments? *Science of The Total Environment*, [online] 563-564, pp.302–319. doi:https://doi.org/10.1016/j.scitotenv.2016.04.094.

Gori, K., Mortensen, H.D., Arneborg, N. and Jespersen, L., 2007. Ammonia production and its possible role as a mediator of communication for Debaryomyces hansenii and other cheese-relevant yeast species. *Journal of Dairy Science*, [online] 90(11), pp.5032–5041. doi:https://doi.org/10.3168/jds.2006-750.

Grimshaw, R.W., 1971. *Physics and chemistry of clay*. LONDON: Ernest Benn Ltd, pp.29–37.

Groudev, S.N., 1987. Use of heterotrophic microorganisms in mineral biotechnology. *Acta Biotechnologica*, 7(4), pp.299–306. doi:https://doi.org/10.1002/abio.370070404.

Guo, M., Lin, Y., Xu, X. and Chen, Z., 2010a. Bioleaching of iron from kaolin using Fe (III)-reducing bacteria with various carbon nitrogen sources. *Applied Clay Science*, 48(3), pp.379–383. doi:https://doi.org/10.1016/j.clay.2010.01.010.

Guo, M.-R., He, Q.-X., Li, Y.-M., Lu, X. and Chen, Z., 2010b. Removal of Fe from Kaolin Using Dissimilatory Fe (III)-Reducing Bacteria. *Clays and Clay Minerals*, 58(4), pp.515–521. doi:https://doi.org/10.1346/ccmn.2010.0580406.

Hajihoseini, J. and Fakharpour, M., 2019. Effect of temperature on bioleaching of iron impurities from kaolin by *Aspergillus niger* fungal. *Journal of Asian Ceramic Societies*, [online] 7(1), pp.82–89. doi:https://doi.org/10.1080/21870764.2019.1571152.

HALVORSON, H.O. and STARKEY, R.L., 1927. *Studies on the transformations of iron in nature. II. Concerning the importance of microorganisms in the solution and precipitation of iron.* Soil Science, pp.381–402.

Hosseini, M.R. and Ahmadi, A., 2015. Biological beneficiation of kaolin: A review on iron removal. *Applied Clay Science*, 107, pp.238–245. doi:https://doi.org/10.1016/j.clay.2015.01.012.

Hosseini, M.R., Pazouki, M., Ranjbar, M. and Habibian, M., 2007. Bioleaching of iron from highly contaminated Kaolin clay by Aspergillus niger. *Applied Clay Science*, 37(3-4), pp.251–257. doi:https://doi.org/10.1016/j.clay.2007.01.010.

Jing, H., Liu, Z., Kuan, S.H., Chieng, S. and Ho, C.L., 2021. Elucidation of Gram-Positive Bacterial Iron(III) Reduction for Kaolinite Clay Refinement. *Molecules*, [online] 26(11), p.3084. doi:https://doi.org/10.3390/molecules26113084.

Jozanikohan, G. and Abarghooei, M.N., 2022. The Fourier transform infrared spectroscopy (FTIR) analysis for the clay mineralogy studies in a clastic reservoir. *Journal of Petroleum Exploration and Production Technology*, [online] 12(8), pp.2093–2106. doi:https://doi.org/10.1007/s13202-021-01449-y.

Koloušek, D., Štyriaková, I., Štyriak, I., Malachovský, P. and Večera, Z., 2007. Bacterial clay release and iron dissolution during the quality improvement of quartz sands. *Hydrometallurgy*, 89(1-2), pp.99–106. doi:https://doi.org/10.1016/j.hydromet.2007.06.002.

Kostka, J.E., Dalton, D.D., Skelton, H., Dollhopf, S. and Stucki, J.W., 2002. Growth of Iron(III)-Reducing Bacteria on Clay Minerals as the Sole Electron Acceptor and Comparison of Growth Yields on a Variety of Oxidized Iron Forms. *Applied and Environmental Microbiology*, 68(12), pp.6256–6262. doi:https://doi.org/10.1128/aem.68.12.6256-6262.2002.

Kumari, N. and Mohan, C., 2021. Basics of Clay Minerals and Their Characteristic Properties. *Clay and Clay Minerals*. [online] doi:https://doi.org/10.5772/intechopen.97672.

LEE, E., CHO, K. and WOOKRYU, H., 2002. Microbial refinement of kaolin by iron-reducing bacteria. *Applied Clay Science*, 22(1-2), pp.47–53. doi:https://doi.org/10.1016/s0169-1317(02)00111-4.

Lee, W., Chieng, S., Lim, S., Yong, S.N. and Kuan, S.H., 2023. Impact of Bacillus species on Fe reduction of kaolin in bioleaching: surface, structural, and chemical studies. *Applied Microbiology and Biotechnology*, 107(15), pp.4789–4801. doi:https://doi.org/10.1007/s00253-023-12622-0.

Mesquita, L., Rodrigues, T.M. and Gomès, S., 1996. Bleaching of Brazilian kaolins using organic acids and fermented medium. *Minerals Engineering*, 9(9), pp.965–971. doi:https://doi.org/10.1016/0892-6875(96)00087-8.

Musial, I., Cibis, E. and Rymowicz, W., 2011. Designing a process of kaolin bleaching in an oxalic acid enriched medium by Aspergillus niger cultivated on biodiesel-derived waste composed of glycerol and fatty acids. *Applied Clay Science*, 52(3), pp.277–284. doi:https://doi.org/10.1016/j.clay.2011.03.004.

Nandakumar, M.P., Sapre, A., Lali, A. and Mattiasson, B., 1999. Monitoring of low concentrations of glucose in fermentation broth. *Applied Microbiology and Biotechnology*, [online] 52(4), pp.502–507. doi:https://doi.org/10.1007/s002530051552.

Mohd, Alias, S., Shakrani, S.A. and Ayob, A., 2024. Structural Order-Disorder Analysis of Thermally-Activated Water-Washed Kaolin Particles Using Fourier

Transform Infrared Spectroscopy. *Engineering chemistry*, 6, pp.45–52. doi:https://doi.org/10.4028/p-10drdd.

Raji, M., Qaiss, A. el kacem and Bouhfid, R., 2020. Effects of bleaching and functionalization of kaolinite on the mechanical and thermal properties of polyamide 6 nanocomposites. *RSC Advances*, 10(9), pp.4916–4926. doi:https://doi.org/10.1039/c9ra10579d.

Rmladmin, 2023. *Difference between Absorbance and Transmittance In FTIR*. [online] Rocky Mountain Labs. Available at: https://rockymountainlabs.com/difference-between-absorbance-and-transmittance-in-ftir/ [Accessed 24 Apr. 2024].

Rymowicz, W., 2003. Oxalic acid production from lipids by a mutant of Aspergillus niger at different pH. *Biotechnology Letters*, 25(12), pp.955–958. doi:https://doi.org/10.1023/a:1024082130677.

Santoro, R., Cameselle, C., Rodríguez-Couto, S. and Sanromán, Á., 1999. Influence of milk whey, nitrogen and phosphorus concentration on oxalic acid production by Aspergillus niger. *Bioprocess Engineering*, 20(1), pp.1–5. doi:https://doi.org/10.1007/pl00009032.

Scorzelli, R.B., Bertolino, L.C., Luz, Arruda, F., P. Munayco and Duttine, M., 2008. Spectroscopic studies of kaolin from different Brazilian regions. *Clay Minerals*, 43(1), pp.129–135. doi:https://doi.org/10.1180/claymin.2008.043.1.10.

Scorzelli, R.B., Bertolino, L.C., Rossi, A.M. and Torem, M.L., 2010. Influence of iron on kaolin whiteness: An electron paramagnetic resonance study. *Applied Clay Science*, 49(3), pp.170–175. doi:https://doi.org/10.1016/j.clay.2010.04.022.

Štyriaková, I., Štyriak, I. and Kušnierová, M., 1999. The release of sulphidic minerals from aluminosilicates by Bacillus strains. *Process Metallurgy*, 9, pp.587–596. doi:https://doi.org/10.1016/s1572-4409(99)80060-1.

Štyriaková, I., Jablonovská, K., Mockovčiaková, A., Bekéniyová, A., Štyriak, I., Kraus, I., Osacký, M. and Lovás, M., 2010. Dissolution of iron from quartz sands by basin bioleaching under static in-situ conditions. *Hydrometallurgy*, 104(3-4), pp.443–447. doi:https://doi.org/10.1016/j.hydromet.2010.03.026.

Štyriaková, I., Mockovčiaková, A., Štyriak, I., Kraus, I., Uhlík, P., Madejová, J. and Orolínová, Z., 2012. Bioleaching of clays and iron oxide coatings from quartz sands. *Applied Clay Science*, 61, pp.1–7. doi:https://doi.org/10.1016/j.clay.2012.02.020.

ŠTYRIAKOVÁ, I., ŠTYRIAK*, I. and MALACHOVSKÝ, P., 2007. Nutrients enhancing the bacterial iron dissolution in the processing of feldspar raw materials. *tyriakova, Iveta and Styriak, Igor and Malachovsky, Pavol}, journal={Ceramics Silikaty*, 51(4), p.202.

ŠTYRIAKOVÁ, I. and ŠTYRIAK, I., 2000. Iron Removal From Kaolin By Bacterial Leaching. *Ceramics-silikaty*, 44(4), pp.135–141.

Štyriaková, I., Štyriak, I., Malachovský, P. and Lovás, M., 2006. Biological, chemical and electromagnetic treatment of three types of feldspar raw materials. *Minerals Engineering*, 19(4), pp.348–354. doi:https://doi.org/10.1016/j.mineng.2005.10.010.

Štyriaková, I., Štyriak, I., Nandakumar, M.P. and Mattiasson, B., 2003. Bacterial destruction of mica during bioleaching of kaolin and quartz sands by Bacillus cereus. *World Journal of Microbiology and Biotechnology*, 19(6), pp.583–590. doi:https://doi.org/10.1023/a:1025176210705.

Tracy, L., 2018. *Factors affecting the whiteness of kaolin*. [online] www.linkedin.com. Available at: https://www.linkedin.com/pulse/factors-affecting-whiteness-kaolin-bubble-jiang/ [Accessed 14 Aug. 2023].

Tsuneda, S., Aikawa, H., Hayashi, H., Yuasa, A. and Hirata, A., 2003. Extracellular polymeric substances responsible for bacterial adhesion onto solid surface. *FEMS Microbiology Letters*, 223(2), pp.287–292. doi:https://doi.org/10.1016/s0378-1097(03)00399-9.

Wenk, H.-R. and Bulakh, A., 2004. Important information about silica materials and feldspars. *Cambridge University Press eBooks*, pp.313–336. doi:https://doi.org/10.1017/cbo9780511811296.021.

Yap, H.J., Yong, S.N., Cheah, W.Q., Chieng, S. and Kuan, S.H., 2020. Bioleaching of Kaolin with Bacillus cereus: Effect of Bacteria Source and Concentration on Iron Removal. *Journal of Sustainability Science and Management*, 15(4), pp.91–99. doi:https://doi.org/10.46754/jssm.2020.06.009.

Yong, S.N., Lim, S., Ho, C.L., Chieng, S. and Kuan, S.H., 2022. Mechanisms of microbial-based iron reduction of clay minerals: Current understanding and latest developments. *Applied Clay Science*, 228, p.106653. doi:https://doi.org/10.1016/j.clay.2022.106653.

Zegeye, A., Yahaya, S., Fialips, C.I., White, M.L., Gray, N.D. and Manning, D.A.C., 2013. Refinement of industrial kaolin by microbial removal of iron-bearing impurities. *Applied Clay Science*, 86, pp.47–53. doi:https://doi.org/10.1016/j.clay.2013.08.041.

Appendix

Sample Day 0	Day 0 element weight %				
	O	Al	Si	K	Fe
Raw 1	47.55	20.04	27.36	3.39	1.65
Raw 2	48.03	19.55	26.49	4.19	1.74
Raw 3	47.24	20.24	27.46	3.36	1.7
Con a	46.42	21.4	27.28	3.01	1.89
Con b	42.85	18.32	29.11	8.01	1.71
Con c	49.51	19.43	26.41	3.11	1.54
BC a	44.04	21.56	29.08	3.81	1.52
BC b	43.4	21.66	28.91	4.45	1.57
BC c	44.2	21.48	28.4	4.26	1.66
BC d	43.91	20.85	29.11	4.59	1.54
BC e	33.78	24.25	34.33	5.89	1.75
BC f	44.03	20.4	27.77	5.99	1.81
Sum					
Raw	142.82	59.83	81.31	10.94	5.090
Con	138.78	59.15	82.8	14.13	5.140
BC	253.36	130.2	177.6	28.99	9.850
Avg					
Raw	47.61	19.94	27.10	3.65	1.70
Con	46.26	19.72	27.60	4.71	1.71
BC	42.23	21.70	29.60	4.83	1.64
Improvement rate (%)					54.88

Day 10	Day 10 element weight %				
	O	Al	Si	K	Fe
Con a	38.98	22.5	30.74	5.59	2.18
Con b	46.8	18.25	27.87	5.19	1.87
Con c	43.82	21.96	28.41	3.83	1.98
BC 1a	48.71	20.86	27.39	2.4	0.64
BC 1b	49.98	20.84	25.44	2.95	0.8
BC 1c	49.67	21.06	26.05	2.42	0.8
BC 2a	50.69	20.9	25.65	2.09	0.67
BC 2b	48.65	22.8	26.75	1.16	0.65
BC 2c	50.89	21.42	25.28	1.64	0.77
BC 3a	51.83	20.16	24.46	2.71	0.84
BC 3b	47.44	20.03	27.91	3.91	0.71
BC 3c	51.55	19.56	25.64	2.42	0.82
Con	129.6	62.71	87.02	14.61	6.03
BC1	148.36	62.76	78.88	7.77	2.24
BC2	150.23	65.12	77.68	4.89	2.09
BC3	150.82	59.75	78.01	9.04	2.37
Con	43.20	20.90	29.01	4.87	2.01
BC	49.93	20.85	26.06	2.41	0.74

Appendix A: The sample of the collected raw data in excel (Batch 1).

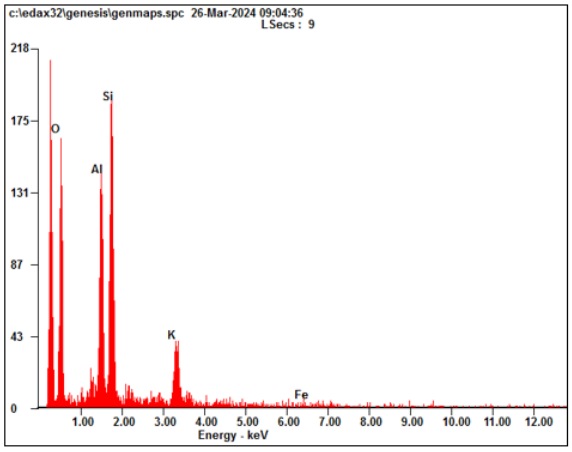

Element	Wt%	At%
OK	43.71	58.71
AlK	18.80	14.97
SiK	27.73	21.22
KK	08.21	04.51
FeK	01.54	00.59
Matrix	Correction	ZAF

Appendix B: EDS results of *B. cereus 4*.

Appendix C: Overnight culture of *B. cereus.*

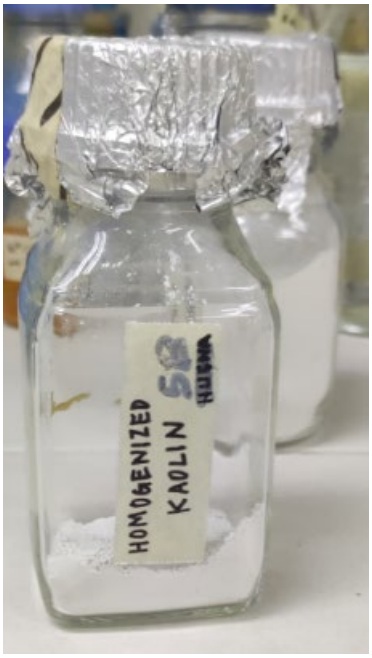

Appendix D: Homogenized kaolin powder.

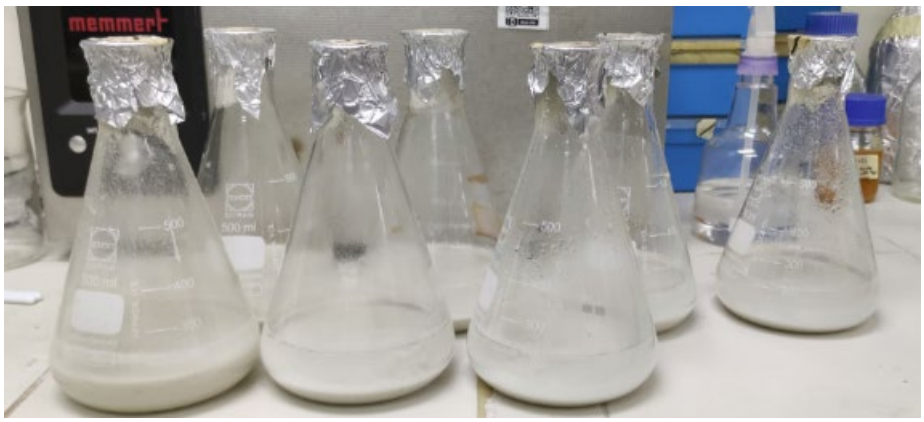

Appendix E: Pure kaolin solution.

Appendix F: Yeast Extract.

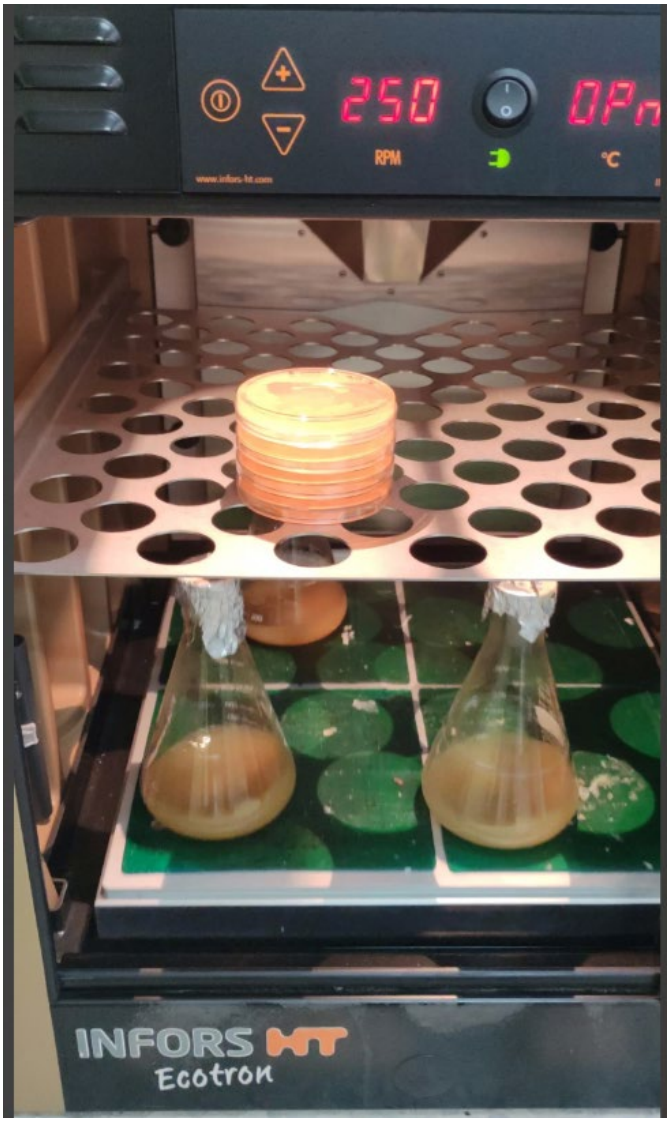

Appendix G: Incubator.

Appendix H: Kaolin suspension.

Appendix I: Filtration.

Appendix J: Membrane filter paper.

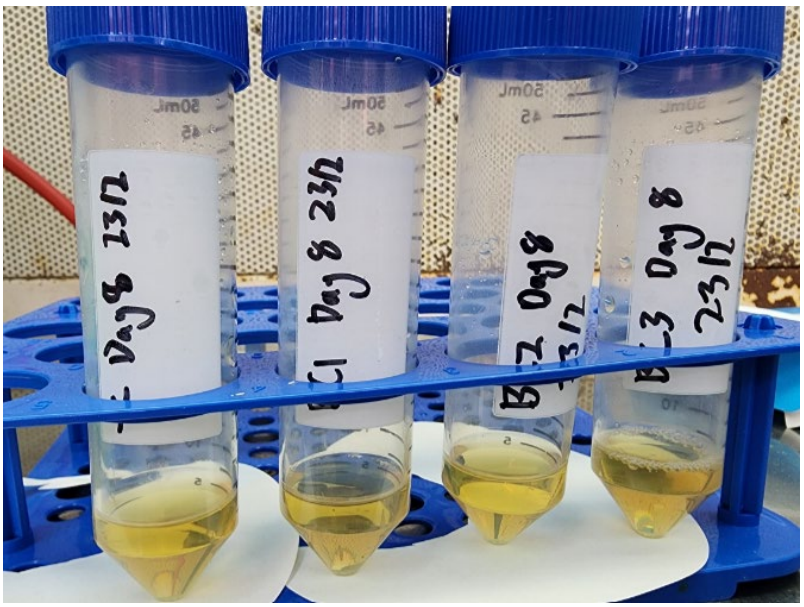

Appendix K: Supernatant.

Appendix L: Precipitate.

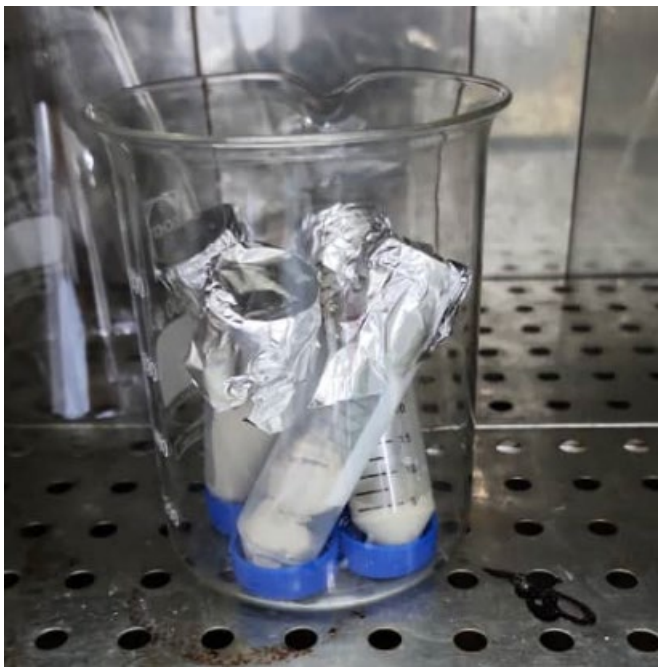

Appendix M: Oven is used to dry the kaolin precipitate.

Appendix N: Cell density meter (Ultrospec 10).

Appendix O: Sample preparation for SEM-EDS.

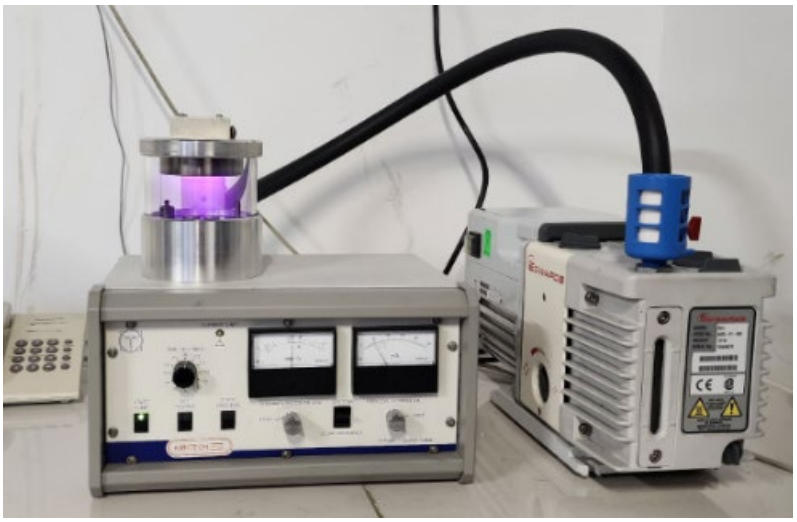

Appendix P: Coating machine for samples before SEM-EDX analysis.